

# Progress and challenges in understanding Asian palaeogeography and monsoon evolution from the perspective of the plant fossil record

ROBERT A. SPICER<sup>1,2</sup> AND ALEX FARNSWORTH<sup>3,4</sup>

<sup>1</sup>CAS Key Laboratory of Tropical Forest Ecology, Xishuangbanna Tropical Botanical Garden, Chinese Academy of Sciences, Xishuangbanna 666303, China.

<sup>2</sup>School of Environmental, Earth and Ecosystem Sciences, The Open University, Walton Hall, Milton Keynes, MK7 6AA, U.K.

<sup>3</sup>School of Geographical Sciences and Cabot Institute, University of Bristol, Bristol, BS8 1SS, U.K.

<sup>4</sup>Key Laboratory of Continental Collision and Plateau Uplift, Institute of Tibetan Plateau Research, and Center for Excellence in Tibetan Plateau Earth Sciences, Chinese Academy of Sciences, Beijing 100101, China.

Email: r.a.spicer@open.ac.uk, alex.farnsworth@bristol.ac.uk

## ABSTRACT

Spicer RA & Farnsworth A 2021. Progress and challenges in understanding Asian palaeogeography and monsoon evolution from the perspective of the plant fossil record. *Journal of Palaeosciences* 70(2021): 213–235.

Land surface elevation, climate and vegetation are intrinsically linked at a range of spatial and temporal scales. In the case of Asia, complex relief hosts some of the richest biodiversity on our planet and is dominated by a system of monsoons, the features of which are determined in large part by topography and land surface characteristics, including vegetation. Such regions have not only acted as an incubator for evolving species but also as refugia during periods of environmental crisis. The exceptional topography of Asia includes the largest and highest elevated region on Earth, the Tibetan Plateau, along with the Himalaya and the Hengduan mountains, collectively referred to here as the THH region. In recent years there has been a revolution in thinking as to how the THH was formed, how the several monsoons systems that affect it have changed, and how it has influenced regional, even global, biodiversity evolution. Accurately dated plant fossils have played key roles in these advances. Here we review the complex evolution of the THH landscape, the modernization of the biota in the Paleogene, and the transition to the modern landscape and monsoon systems in the Neogene. We show how these changes in understanding have been brought about by recent fossil discoveries and new radiometric dating of previously known assemblages, methodological advances arising from integrating improved proxy data, and numerical palaeoclimate modelling. Significant knowledge gaps remain, however, which demand further advances in proxy and numerical methodologies, as well as new fossil discoveries in key locations for specific time intervals.

**Key-words**—Tibet, Himalaya, Palaeoaltimetry, Plant fossils, Palaeoclimate

## INTRODUCTION

NUMEROUS papers attempt to link the Indo–Eurasia collision and the Tibetan–Himalayan orogeny to changing monsoon dynamics and biodiversity evolution, often based on nothing more than supposition and a poor understanding of how these events fit together in time and space. For example, many papers on molecular phylogenetics have (wrongly) ascribed Miocene diversification events within Asia to the 'uplift of the Tibetan Plateau' and monsoon development (reviewed in Renner, 2016). We can say with

confidence that this is wrong because recent work has demonstrated that there was no such thing as the uniform rise of a pre-formed plateau (Spicer *et al.*, 2020 a, b) and that although plateau formation had taken place by the Miocene much of the orogeny occurred in the Paleogene (Ding *et al.*, 2014; Su *et al.*, 2020; Spicer, 2017; Spicer *et al.*, 2020a–c) but not, we now know, as envisaged by Renner (2016) either. New and more numerous proxy discoveries (e.g. Lin *et al.*, 2020; Su *et al.*, 2019; Zhuang *et al.*, 2019), better age determination (Gourbet *et al.*, 2017; Linnemann *et al.*, 2018; Tian *et al.*, 2021) and a reduction in methodological uncertainties (e.g.

Farnsworth *et al.*, 2021) are allowing greater insights into the topographical evolution of this region. This is a fast-moving field. Moreover, the presence of Asian monsoon climates long predates the Cenozoic and modernization of the Asian biota, at least that associated with the Tibetan region, mostly took place in the Paleogene.

In the last five years there have been substantial advances in our understanding of topographic development across the Tibetan region (e.g., Spicer *et al.*, 2020c), the emergence of monsoon systems with modern characteristics (Bhatia *et al.*, 2021 a, b; Farnsworth *et al.*, 2019; Spicer *et al.*, 2017), and when Asian biotas assumed their modern compositions (Li *et al.*, 2021; Linnemann *et al.*, 2018; Tian *et al.*, 2021). These new insights have arisen from new fossil finds (Su *et al.*, 2019; 2020), and revised absolute dating of previously known fossil biotas (Li *et al.*, 2020; Linnemann *et al.*, 2018; Tian *et al.*, 2021), while advances in methodologies (Valdes *et al.*, 2019; Li *et al.*, 2021; Farnsworth *et al.*, 2021) are enabling us to quantify past land surface height with greater precision, and re-evaluate the assumptions underlying data exploration and interpretation (Spicer *et al.*, 2020a–c). In this contribution we will bring together some key discoveries and throughout we highlight gaps in our knowledge that, if filled, could advance our understanding further. The ideas we summarise here may also be short-lived due to new advances, so this is just a snapshot of the current 'state of play'. Our focus will mostly be on the Cenozoic, but Mesozoic monsoons affecting India are also considered as they set the stage for what followed.

## MONSOONS

Monsoons are a major feature of the modern climate system and theoretically should have existed in one form or another throughout Earth's history (Acosta & Huber, 2020), provided that Earth's obliquity has remained similar to that of the present day (Webster & Fasullo, 2003). However, despite their importance and persistence through time there is a great deal of confusion as to what the term 'monsoon' means and how it should be defined quantitatively. The word 'monsoon' is derived from the Arabic word "mausim", meaning a seasonal wind. Early monsoon definitions relied solely on a seasonal wind reversal ( $>120^\circ$ ) (Ramage, 1971), however, this effectively removed South America as having a monsoonal climate due to it having no such seasonal wind reversal. To some it just means intense rainfall and, although this is equally wrong, abundant seasonal variation in precipitation is a common feature of monsoons. Even for the present day there are many different monsoon definitions, and this is confusing. To define a monsoon, and in particular to characterise different monsoon types, requires complex meteorological metrics involving atmospheric pressure, wind directions and rainfall patterns, often expressed in terms of average daily precipitation as measured over at least 30 years (e.g. Wang & Ho, 2002; Zhang & Wang, 2008). These

metrics are not preserved in their entirety in the rock record, so tracking monsoon evolution through time has to be done using proxies that preserve only some of these characteristics and so inevitably fail to capture the complexities of modern monsoon characterizations (Spicer *et al.*, 2016).

The Asian landscape (here meaning topography and vegetation) and its monsoons are intrinsically linked: monsoons climates having contributed to landscape erosion and increases in relief (Nie *et al.*, 2018) and niche heterogeneity which, combined with climate variation, drives speciation (Antonelli *et al.*, 2018; Rahbeck *et al.*, 2019; Spicer, 2017, 2020a).

A monsoon system across southern Asia today is inevitable because in its present location it intrudes into the global Inter-tropical Convergence Zone (ITCZ) rain belt, which in the modern world extends to approximately 25–28° latitude over the oceans (Wang & Ho, 2002; Zhang & Wang, 2008). The latitudinal bounds of this rain belt and its longitudinal continuity are modified by the presence of land masses, with Asia seeing the most extreme poleward extension of the monsoon to  $>40^\circ\text{N}$  (Fig. 1). This otherwise low latitude global ITCZ monsoon belt exists due to seasonal latitudinal oscillations of the thermal equator between the tropics of Cancer and Capricorn. Associated with this moving thermal equator is a band of convective rainfall that permanently overlaps itself to form a narrow 'ever-wet' zone centred on the geographical equator (Fig. 1). How wide this ever-wet zone has been in the past, and the latitudes between which the thermal equator has migrated, has depended on small changes in Earth's obliquity, large-scale circulation (the strength and location of the Hadley–Walker circulation), ocean circulation and regional sea surface temperatures, and the strength of the polar high–pressure cells, which in turn are dependent on polar temperatures and the equator–to–pole temperature gradient. The coherence of this belt also depends on land–sea thermal contrasts determined in large part by the disposition of the continents (Fig. 1)

The present-day position of southern Asia within this ITCZ migration range also means that the presence of a monsoon system over parts of Asia is not solely dependent on an elevated Tibet or Himalaya (Acosta & Huber, 2020). The size alone of the Asian continent is enough to distort the normal ITCZ latitudinal range because in the summer the northern boundary of the ITCZ migration is drawn poleward due to a strong low–pressure system centred over Central Asia as a result of continental interior sensible heat flux. In winter, pronounced cooling over the same region creates a high–pressure cell and some descending cold dry air travels south–eastwards, influenced by the westerlies, to affect large parts of northern China. The strength of the central Asian pressure oscillation also depends on the overall global thermal regime.

The questions we are considering here do not encompass whether or not there have been monsoons over Asia in deep time, undoubtedly there were. Instead we focus on what we

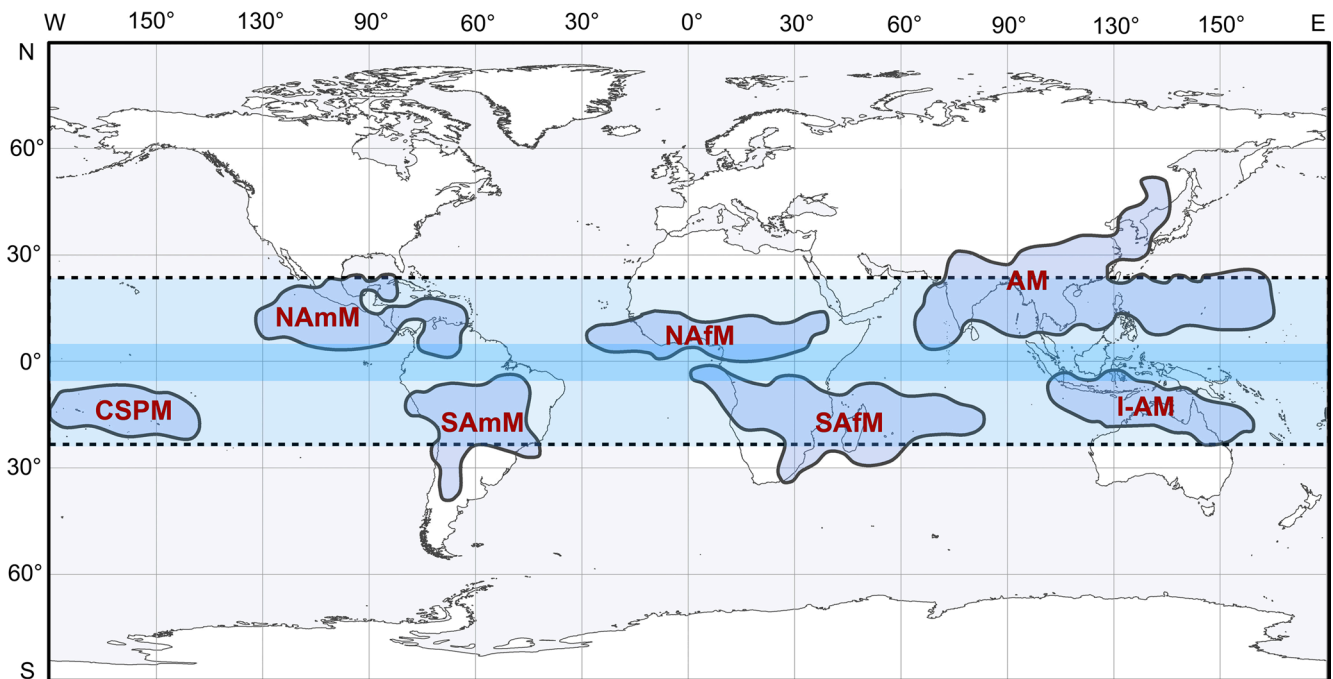


Fig. 1—Present-day map of global monsoon systems based on Zhang & Wang (2008): CSPM—Central Southern Pacific Monsoon, NAmM—North American Monsoon, SAmM—South American Monsoon, NAfM—North African Monsoon, SAfM—South African Monsoon, AM—Asian Monsoon, I-AM—Indonesia–Australia Monsoon. Dotted lines indicate the approximate poleward seasonal migration of the rain belt associated with the Inter-Tropical Convergence Zone (ITCZ) in a theoretical world devoid of continents but with Earth's present obliquity. The equatorial darker blue band indicates the ever-wet zone where the ITCZ rain belt would permanently overlap in such a theoretical world. Note that this is an idealized depiction, even in a world devoid of land masses ocean circulation and thermal heterogeneity associated with that circulation would distort these rainfall bands.

know about the evolution of the Asian landscape and biota and their interactions with monsoon patterns. In complex systems such as we are considering here it is difficult to link cause and effect, and in the past researchers have been all too eager to make extravagant claims of causality based on very few data points in time and space. Unsurprisingly this has led to claim, counter claim and confusion. In the case of India, its rapid movement north–eastwards across the equator further complicates making generalities about monsoon influences over time. First, we take a step backwards and examine the interactions between India and the ITCZ monsoons during its northward journey.

### Ancient Monsoons

Deep time (Kimmeridgian ~155 Ma.) numerical climate modelling (Armstrong *et al.*, 2016) (Fig. 2) shows the long-term persistence of the ITCZ monsoon belt, and how this belt becomes distorted by land–sea thermal contrasts (both regionally and hemispherically). At ~155 Ma the continents were aggregated into the giant supercontinent, Pangea, that took the form of a letter 'C' straddling the Equator (Fig. 2). In the Northern Hemisphere the land mass was fragmented at low latitudes by the developing Tethys seaway, so the ITCZ rain belt was not expanded polewards as much as it was in the

Southern Hemisphere where no such fragmentation existed. This pronounced southward distortion is analogous to that experienced today over Asia, where a large continental mass develops its own seasonal oscillating pressure system because of its size and position spanning mid latitudes. At 155 Ma, only what is now SE Asia was positioned within the northern ITCZ zone, while all of what is now left of the Indian Plate after subduction of 'greater India' was located south of the southern ITCZ monsoon belt.

By the beginning of the Cenozoic virtually all of India must have moved into the ITCZ monsoon belt, and in so doing changed the ITCZ characteristics. For most of the Cretaceous large parts of India must have experienced a monsoonal climate as it tracked through this ITCZ zone, but the extent of India's monsoon exposure will have depended on the details of its motion and interactions with the ITCZ system. This suggests that from early in the Cretaceous onwards the only non-monsoonal climate India may have experienced was when it tracked through the equatorial ever-wet zone, but this zone may not have been very wide if the ITCZ latitudinal migration was greater than now, or the oscillating rain belt associated with the thermal equator was narrower. Recent work has thrown some light on this topic and we shall consider it later.

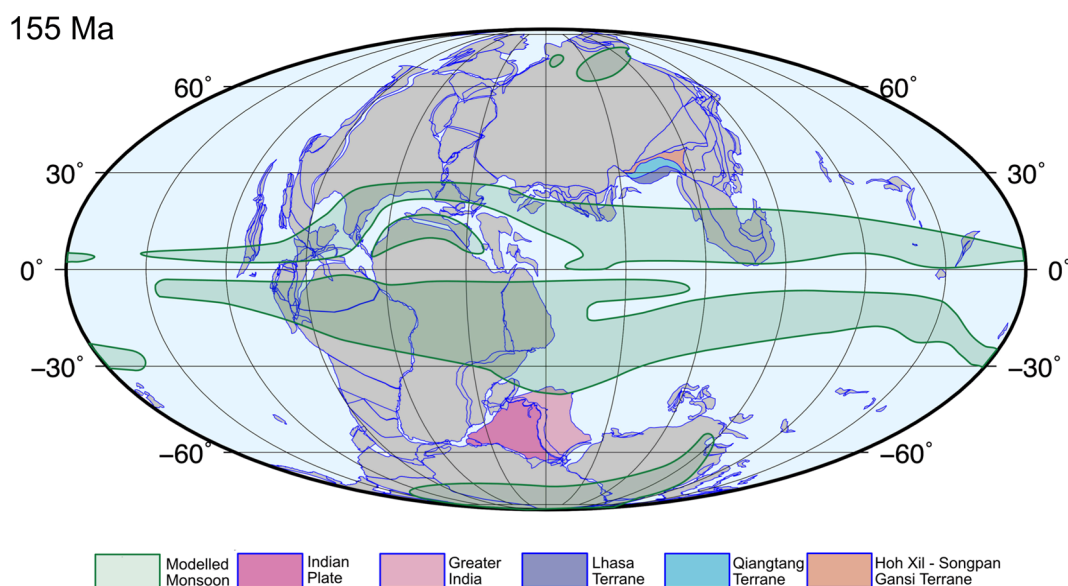


Fig. 2—Map showing past monsoon belts as generated by climate modelling. Modified from Armstrong *et al.* (2016). The Indian Plate and allochthonous Gondwanan terranes that today comprise the Tibetan Plateau are highlighted.

### Geographic and topographic influences on Asian monsoon characteristics

Several modelling studies have demonstrated the long-term persistence of Asian monsoons throughout the late Mesozoic and Cenozoic (e.g. Huber & Goldner, 2012; Farnsworth *et al.*, 2019), and the dominance of palaeogeography and topography over atmospheric  $p\text{CO}_2$  levels in determining monsoon characteristics, particularly over east Asia (Farnsworth *et al.*, 2019). Continental positions, the opening and closing of ocean gateways and bathymetry all affect ocean circulation, and thus heat distribution and the ITCZ seasonal excursions, while on land topography seems to have had the most effect on monsoon intensity (Farnsworth *et al.*, 2019).

Topography exerts two kinds of atmospheric forcing: mechanical (deflecting and blocking of air flow) and thermal (sensible and latent heat fluxes). In the modern world mechanical forcing is strong over Asia due to its extreme and complex topography, importantly orientated in an east–west trending direction. Tropospheric westerly air flow across Asia is deflected and separated by both the Iranian Plateau and the Tibetan Plateau, as well as mountain systems such as the Tien Shan (Fig. 3). In summer, moist air from the Indian Ocean is drawn north–eastwards across India in part by the central Asian (Siberian) low pressure system, in part by a low generated by mid troposphere (850 hPa) heat centred over north–western India and Pakistan (Molnar *et al.*, 2010), and in part by the anomalous heating over the high (~ 5 km) Tibetan Plateau. Much of this air flow is deflected by the even higher (mean elevation ~ 6km) Himalaya, which also blocks

cooler air coming from the north, and which contributes to the anomalous heating over Pakistan and NE India (Molnar *et al.*, 2010). Moist air is also drawn north–eastwards towards the plateau over China from the Pacific and the South China Sea unhindered by the Westerlies, which are blocked by both the plateau itself and the Hengduan Mountains, which extend down into Yunnan (Figs. 3 and 4).

Mechanical forcing also played a roll in determining the past strength and location of the monsoon (Boos & Kuang, 2010; Farnsworth, *et al.* 2019) through regional airmass modification. Topographic barriers such as the predominantly east–west oriented Gangdese inhibited dry–cool central Asian continental air flowing south into ITCZ monsoon regions before the rise of the Himalaya and moderated the flow of warm moist air moving northward.

In the context of the Asian monsoon, thermal forcing takes two forms. For a long time the Tibetan Plateau has been regarded as an anomalous high altitude sensible heat source due to the elevated land surface heating up more in the summer than free air would do at an equivalent altitude, and that this summer heating generates a strong low pressure system (Flohn, 1968; Yanai & Wu, 2006). As mentioned earlier, that idea has been challenged (Molnar *et al.*, 2010), but only in the sense that it is not the primary location of atmospheric heat; the anomalous heat over Pakistan and north–western India being the other. This low–pressure system is present regardless of regional topography (Acosta & Huber, 2020), although monsoon rainfall is weakened over the Indian Continent if the topography is low.

Additional atmospheric heating occurs during the release of latent heat when moisture condenses to form rain.

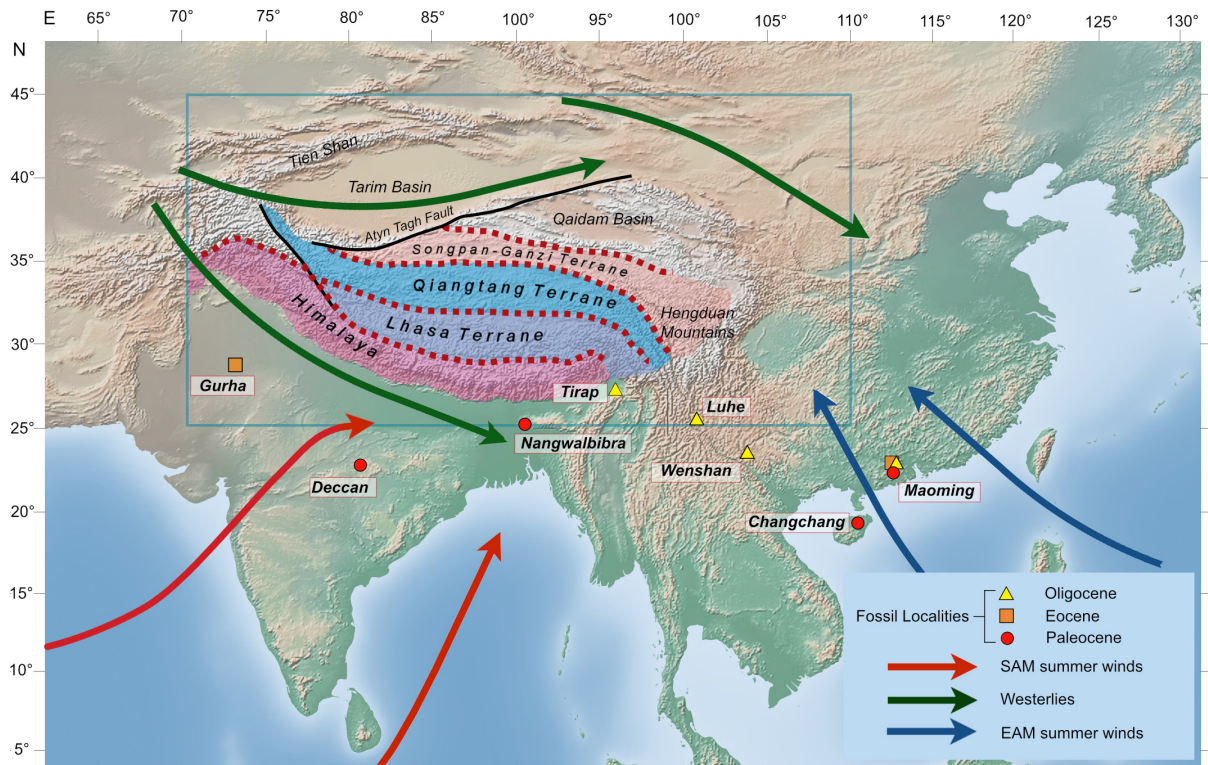


Fig. 3—Map of Asia showing the main seasonal air-flows that comprise the monsoon system. Plant fossil localities referred to in the text are also shown. Details within the blue rectangle are presented in Fig. 4.

In summer this mostly occurs today over north–eastern India and south–eastern Tibet. This heating further intensifies local convection and rainfall.

In the past a warmer atmosphere would have held more moisture, a well-known relationship as expressed by the Clausius–Clapeyron relation (+7% atmospheric water holding capacity per 1°C warming), which would have resulted in more rainfall (roughly ~3%/°C warming due to static stability constraints), and so more intense local heating of the atmosphere when latent heat was released during condensation. Such an increase in latent heat thermal forcing and volatility in the precipitation regime is likely to occur in the future (Ha *et al.*, 2020).

Monsoon rainfall also requires moisture sources. As far as Asia is concerned today those sources are the Indian Ocean, including the Bay of Bengal, the South China Sea and the Western Pacific. In the past, additional sources would have been the Paratethys to the west of central Tibet and the Neotethys between India and Eurasia. Accurate palaeogeographic reconstructions (continental positions, topographic heights, extents, oceanic gateways), including all available moisture sources such as oceans, lakes and evapotranspiration from vegetation, are critical to understanding past thermal and mechanical forcings.

### The Monsoon History of India

Figure 2 suggests that India began to experience monsoon climates soon after it broke away from Gondwana and began its migration northwards, and by the middle Cretaceous (~100 Ma) large parts of the now subducted 'Greater India' were located in the southern ITCZ monsoon rain belt. The size of Greater India is still actively debated as the recent review of Kapp and DeCelles (2019) demonstrates, and the monsoon impact on India depends on how accurately the subcontinent is positioned latitudinally over time.

The onset of continental collision occurs when all oceanic lithosphere between two continental margins has been consumed, the margins come into contact, and subduction of continental crust begins. In the case of the India–Eurasia collision the situation is complicated by the incorporation of the Kohistan–Ladakh Island Arc (Chatterjee *et al.*, 2013), which may have served as a stepping stone for biotic exchange between Africa and India, if not Eurasia, during the Cretaceous (e.g. Chatterjee & Scotese, 2010; Khan *et al.*, 2009, 2020; Sahni, 1988). Such an exchange compromises the use of fossil and molecular phylogenetic evidence for dating plate contact and consequently the time at which this contact took place has long been debated. Estimates range from ~65 Ma (e.g. Ding *et al.*, 2005) to ~22 Ma (van Hinsbergen *et al.*,

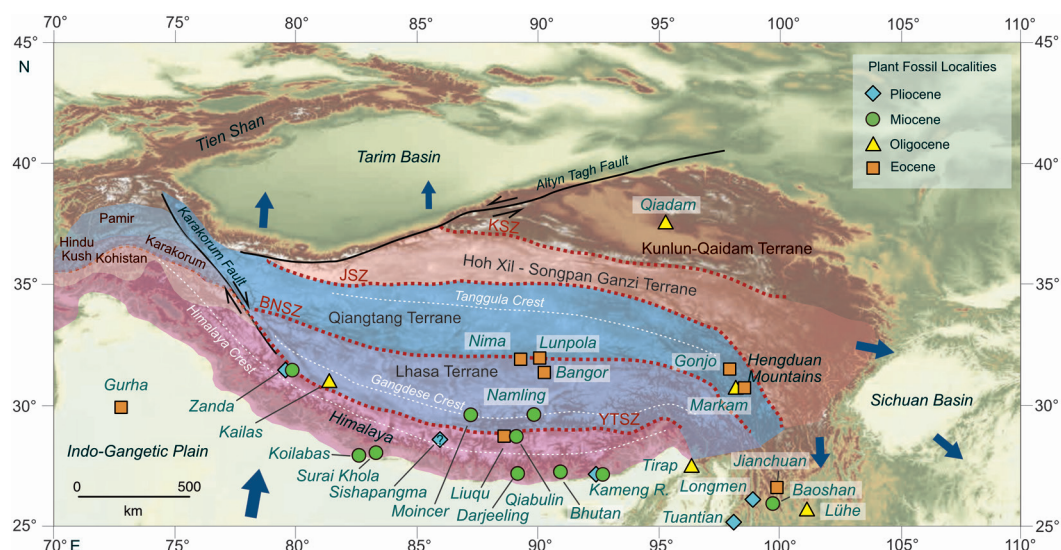


Fig. 4—Map of the Tibetan, Himalaya and Hengduan Mountains (THH) Region showing its component terranes, major sutures and faults. Symbols represent known plant fossil localities of different ages. Blue arrows represent the direction and rate of modern motion measured by GPS. The larger the arrow, the faster the movement.

2012), with most authors favouring  $55 \pm 10$  Ma (Wang *et al.*, 2014). A recent study based on sediment provenance shifts recorded in surviving successions in the central northern Himalaya appears to show that parts of continental greater India were in very close proximity to Eurasia no later than  $\sim 61$  Ma (An *et al.*, 2021), but because the size of greater India is poorly quantified this signal of initial contact does not fully constrain the palaeolatitude of those parts of the Indian Plate that remain today.

Traditionally, tracking India's position through time has been done using palaeomagnetism (e.g. Molnar & Stock, 2007), but a major discrepancy exists between the perceived convergence based on such measurements ( $\sim 4000$  km) and the estimated amount of upper crustal shortening ( $\sim 2000$  km). Some authors have invoked additional ocean basins (e.g. van Hinsbergen *et al.*, 2012; Kapp & DeCelles, 2019) to reconcile the difference, but An *et al.* (2021) argue for a reassessment of palaeomagnetic methodology and questions are now being raised about the reliability of existing measurements used to quantify the size of greater India (Roperch & Dupont-Nivet, 2021). If we assume 2000 km of greater India has now disappeared, and that the An *et al.* (2021) date of first contact (no later than  $\sim 61$  Ma) is correct, it positions the northern edge of what is now the central Himalaya at  $\sim 10^\circ\text{N}$  at  $\sim 61$  Ma, and that at 65 Ma the plants represented in the Deccan plant locality shown in Fig. 3 should have been within the equatorial ever-wet zone, if it existed, and this should be detectable in the fossil record, but at present there are great uncertainties surrounding the details of India's northward journey.

As India continued its journey northwards it would have traversed through the northern ITCZ monsoon zone, perhaps modifying the monsoon as it did so. To detect the kind of

monsoon that different parts of India were exposed to we can use fossil leaf form (Spicer *et al.*, 2016, 2017).

## PLANT FOSSILS AND CLIMATE

The relationship between climate, plant distribution and plant form has been appreciated for more than 2000 years, but has only been reliably quantified and applied to plant fossils within the last few decades (reviewed in Spicer *et al.*, 2020d). Two different approaches have emerged; one based on the climatic tolerances of perceived nearest living relatives (NLRs) of the fossils (e.g. Chevalier *et al.*, 2014; Greenwood *et al.*, 2003, 2005; Kershaw, 1996; Kershaw & Nix, 1988; Mosbrugger & Utescher, 1997; Utescher *et al.*, 2014), and one based on plant form (physiognomy), particularly leaf morphology (e.g. Kovach & Spicer, 1996; Spicer *et al.*, 2020d; Wolfe, 1979, 1993; Yang *et al.*, 2011, 2015). Both methods are capable of estimating thermal (mean annual temperature and cold and warm extremes) and hydrological variables (precipitation, humidity). However, both have their individual strengths and weaknesses, and so where possible should be used in tandem to obtain reliable palaeoclimate and palaeoaltitudinal reconstructions.

NLR techniques require accurate taxon identification and due to evolutionary changes within plant lineages reliability declines the further back in time they are applied (Utescher *et al.*, 2014). Nevertheless, their big advantage is that they can be based on any identifiable plant parts, such as pollen, fruits and seeds, wood, etc. as well as leaves. On the other hand, physiognomic techniques are independent of taxonomy, tend to be more time-stable because they are rooted in the laws of physics and chemistry, but can only be applied to plant organs

whose growth form is modified by the environment (primarily leaves and wood).

Although NLR techniques can return temperature and rainfall data, the usual constraints apply as to how these individual climate metrics properly characterise monsoon regimes in all their complexity. Moreover, because NLR approaches can be applied to highly recalcitrant plant parts such as woody material, pollen and spores, these can potentially be dispersed over far greater distances than leaves, which reduces spatial specificity, including palaeoaltitudinal precision. In the case of pollen/spores, multiple cycles of reworking are also possible, which also reduces temporal precision.

Leaves, particularly those of woody dicots, have to be well adapted to their immediate atmospheric environment or they will not function efficiently. In extreme cases maladapted leaves could lead to plant death and elimination from a community by compromising the fitness on the parent plant. Consequently, macroscopic leaf adaptations exhibited by aggregations of species reflect well the conditions under which those plants grow (Spicer *et al.*, 2020d; Wolfe, 1993; Yang *et al.*, 2011, 2015), and if preserved as fossils these adaptations allow us to reconstruct past climates, including monsoon characteristics (Bhatia *et al.*, 2021a, b; Spicer *et al.*, 2016, 2017;). The most widely used and tested method for doing this, and the one that returns the most climate variables, is known as CLAMP (Climate–Leaf Analysis Multivariate Program—<http://clamp.icas.ac.cn>), the methodology and developmental history of which is reviewed in Spicer *et al.* (2020d) and will not be described in detail here.

CLAMP is currently capable of returning 24 different climate variables spanning temperature, humidity and precipitation (Spicer *et al.*, 2020d). The precipitation estimates are inevitably buffered by moisture available in the soil, which in many instances not only reflects rainfall but proximity to groundwater reserves that may be fed by lakes and rivers whose catchments may extend over thousands of km<sup>2</sup> and large ranges in elevation. If fed by glaciers, the available water may not reflect precipitation contemporaneous with the lifespan of the plant, but water accumulated over millennia. This problem of an allochthonous water supply is true for any plant–based climate proxy, but it does mean that quantitative precipitation estimates have to be viewed with some caution, and this extends to wet: dry season differences and hence monsoon indices (e.g. Liu & Yin, 2002; Xing *et al.*, 2012). Such ratios can be useful in comparative studies within the context of the same methodology, including with the same calibration, but should not be treated as equivalent to ratios derived from direct rainfall measurements.

A better metric is one that is related to moisture in the atmosphere, particularly vapour pressure deficit (VPD), which is critically important to plant growth and is currently rising in a warming world (Grossiord *et al.*, 2020). VPD is a measure of how much pressure moisture in a parcel of air exerts against

further moisture uptake, such that as from transpiration. High VPD leads to water stress in plants, while very low VPDs impede transpirational water loss and movement of nutrients through the plant body. It is therefore no surprise that plants display leaf form adaptations that reflect annual and seasonal variations in VPD (Bhatia *et al.*, 2021a, b; Spicer *et al.*, 2019, 2020d), and this may yet prove a more reliable monsoon indicator than estimated precipitation variables alone. CLAMP regressions indicate that VPD is more precisely correlated with leaf form in wet regimes than dry, and so is different to precipitation where leaf form tends to be more tightly constrained in dry regimes (Spicer *et al.*, 2020d). As yet there are no universal VPD descriptors of monsoons, so a better way is to look directly at leaf trait spectra as expressed under exposure to different modern global monsoons as a way of 'fingerprinting' monsoon characteristics.

### Monsoon 'fingerprinting' using leaf fossils

Leaves have to be adaptive over their entire lifespan, which for many evergreen low latitude taxa can be several years. Consequently, leaf architecture has to confer fitness throughout annual monsoon extremes of temperature, rainfall and evaporative stress, and as a result leaves exposed to monsoon conditions display unique trait spectra that can be used to characterise different monsoon regimes (Fig. 5). Using this approach Bhatia *et al.* (2021a, b) demonstrated India's persistent exposure to predominantly ITCZ type monsoons until the latest Oligocene when leaf trait spectra showed a distinct shift towards the characteristics displayed by the modern SAM (Fig. 5 A–D). Whether this was a result of India moving into a SAM–like monsoon that was already developed over Paleogene Eurasia, or whether the SAM was being generated by India's approach to Eurasia and the start of significant uplift of the Himalaya, has yet to be resolved. Moreover, the CLAMP training (calibration) database of 424 modern vegetation sites worldwide does not yet contain leaf traits from cool locations exposed to the SAM, and as such cannot distinguish a SAM monsoon signature from that expressed by leaves exposed to the EAM at latitudes < ~ 28° N (Fig. 5 A–C). Additional collecting of modern leaves growing at high elevations in the Himalaya may help rectify this shortcoming.

### PALAEOALTIMETRY

Changes in land surface height are measured relative to some datum and ideally that datum is mean sea level, preferably the geoid. In the modern world, before satellite laser or radar methods, elevation differences were measured directly by surveying using trigonometry or by employing some relative change in a physical property such as air pressure. For palaeoaltimetry, estimating air pressure is difficult, although attempts have been made either for the

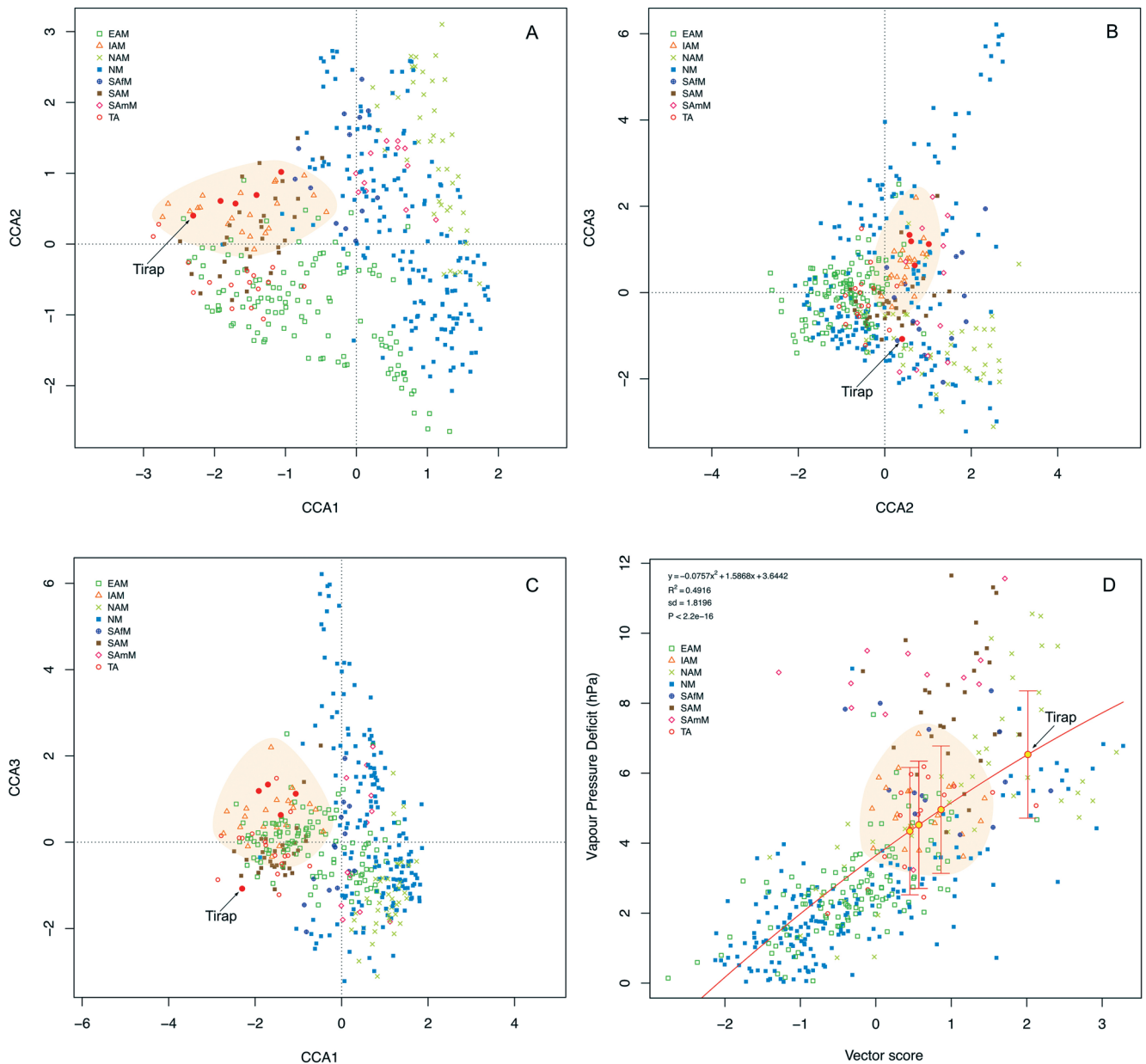


Fig. 5—CLAMP (Canonical Correspondence Analysis) of 424 modern vegetation sites coded for the monsoon climates they grow under (EAM—East Asia Monsoon, IAM—Indonesia–Australia Monsoon, NAM—North American Monsoon, NM—non–monsoon, SAfM—South African Monsoon, SAM—South Asia Monsoon, SAmM—South American Monsoon, TA—Transitional Area). Red filled circles represent the positions of Indian Paleogene fossil sites. A) Axes 1 v2, B) Axes 2 v 3, C) Axes 1 v 3. Only the latest Oligocene Tirap site plots away from modern sites exposed to the ITCZ–type Indonesia–Australia monsoon, highlighted by the orange area. B and C show Tirap plots nearer to sites exposed to the SAM, EAM and TA. D) Winter vapour pressure deficit regression showing that Tirap experienced far drier winter conditions than the other fossil sites, and distinct from conditions experienced today by the Indonesia–Australia monsoon.

atmosphere as a whole (e.g. Sahagian & Maus 1994; Sahagian *et al.*, 2002) or atmospheric components such as the partial pressure of carbon dioxide ( $ppCO_2$ ) (McElwain, 2004). In the case of  $ppCO_2$  estimates this is done using changes in stomatal characteristics (density) because  $ppCO_2$  decreases with increasing elevation, but as with all stomatal responses to  $CO_2$  it is highly species dependant (e.g. Poole *et al.*, 1996; Zhang

*et al.*, 2012), and so limited by species longevity. This causes problems in palaeoaltimetry because of the long timescales ( $\gg 1$  Myrs) over which orographic change takes place. For palaeoaltimetry, changes in other physical parameters are more often employed, with those parameters being derived from geological proxies. These proxies are usually based on isotopes or fossils.

## Isotopes

Potentially there are two ways of determining past surface height using stable isotopes. The first is based on the differential fractionation of heavy and light isotopes, typically oxygen and hydrogen (Mulch, 2016; Mulch & Chamberlain, 2006, 2018; Rowley *et al.*, 2001; Rowley & Garziona, 2007), that takes place as moisture condenses during air parcel ascent and cooling. The second is based on using isotopes to determine land surface temperature from which height can be calculated using thermal lapse rates.

As a parcel of air rises the pressure decreases, it expands, cools and moisture condenses to fall as rain. Heavy isotopes tend to rain out more than light isotopes (Rowley & Garziona, 2007). This means that rain at increasing elevations on the windward side of a mountain range will contain decreasing amounts of the heavy isotope and moisture passing over the mountain ridge will be enriched in the lighter isotopes relative to when it started its ascent. In such a simple scenario the pattern of isotopic change with increasing elevation (the isotopic lapse rate) is broadly predictable using a Rayleigh condensation model. Preferential rainout of heavy isotopes also occurs as air rises through convective processes high above any land surface, but this is usually ignored, perhaps wrongly, in this approach. The isotopic composition at a known elevation (usually sea level) at the start of the air parcel ascent also needs to be known.

To be useful as a palaeoaltimeter the isotopic ratio of meteoric water needs to be captured in a carrier material, typically a mineral or organic matter, and preserved, diagenetically unaltered through time, along with similar contemporaneous data from a location at the start of the air parcel trajectory. The residence time of meteoric water in the groundwater system, or as glacier ice, before it is preserved in a carrier can be of concern because the longer the residence time the further that water can travel downslope before being fixed in the carrier, and the greater the chance that the isotopic ratios may be altered from those at condensation. Residence times can also increase temporal uncertainty. Inevitably, such stable isotope palaeoaltimetry results will be biased towards the elevations at which limiting isotope fractionation takes place, that is to say above mountain range ridges, and be subject to multiple cycles of evapotranspiration and condensation as an air parcel traverses land surfaces from its origin and before its final ascent. This introduces a so-called 'continental effect' (Mulch, 2016; Mulch & Chamberlain, 2006, 2018) that is difficult to quantify without using isotope-enabled numerical Earth system models with realistic boundary conditions, including prescribed ancient topography (e.g. Xiong *et al.*, 2020).

Stable isotopes can also be used to determine land surface temperatures and, by using thermal lapse rates (see below), these can be used to estimate surface height. To avoid

complications due to differential isotope fractionation such temperatures are increasingly being obtained from so called 'clumped isotopes'. Clumped isotopes reflect how the isotopes are arranged in the mineral crystal lattice of the carrier, and specifically involve molecules of similar composition but made up of different isotopes (isotopologues). The most common clumped isotope palaeothermometer measures the isotopologues of carbon and oxygen in CO<sub>2</sub> with a mass of 47 when it is released from carbonates as they are dissolved in phosphoric acid, i.e. when <sup>13</sup>C and <sup>18</sup>O are substituted for <sup>12</sup>C and <sup>16</sup>O. The amount of 'clumping' ( $\Delta_{47}$ ) is temperature dependant (Ghosh *et al.*, 2006; Eiler 2007, 2011), with preferential clumping of the heavier isotopes (<sup>13</sup>C and <sup>18</sup>O) taking place at lower temperatures, although disequilibrium and 'vital' effects introduced by biochemical reactions do occur (Affek *et al.*, 2008; Zaarur *et al.*, 2011).

For this approach to be reliable the isotopes at both the reference location for which the elevation is known (usually sea level) and that at the unknown (usually at some elevated location) have to reflect accurately the temperature at which their carrier materials form, and this temperature depends on the nature of the carrier material and whether or not carrier formation is biased towards one season or another. Low elevation sites can experience a warmer, wider range and longer duration of formation temperatures than those at higher (colder) elevations when carrier formation may be more prevalent during the warmer months (Quade *et al.*, 2013). At higher elevations summer glacial melting can also cool rivers, lakes and groundwater in which some of the isotope carriers such as gastropod shells or sub-aqueous carbonates form (Huntington *et al.*, 2015). Similarly, soil carbonates can be dependent upon the moisture regime, so the time when such carrier material forms is not just a function of temperature (Gallagher & Sheldon, 2016). Carbonate palaeosol nodules only form when the soil is moist but drying, and so is a function of a lack of rainfall combined with high evapo-transpiration, which in turn depends on vegetation type and density (Gallagher & Sheldon, 2016). Vegetation also affects soil surface temperatures through shading (Quade *et al.*, 2013), so ideally plant fossils are required to characterise such palaeovegetation. Moreover, soil carbonate nodules can take several thousand years to form (Retallack, 2005), so smoothing out and potentially biasing thermal variations as a function of orbitally-driven climate and vegetation change.

Inevitably the numerous assumptions and complex processes involved in isotope palaeoaltimetry make its application difficult in complex landscapes such as those that comprise the Tibetan region. Heterogeneous landscapes in turn give rise to complex climate patterns through mechanical and thermal forcing, so quantifying topographic variation becomes extremely problematic unless conducted within a rigorous modelling framework. So far, such an approach is the exception rather than the rule.

### Plant fossils

Plant megafossils, such as leaves, record adaptations to climate expressed by vegetation that equilibrates to its immediate environment over much shorter time intervals than it takes for soil carbonate nodules to form (a few centuries at most, but often less). Moreover, leaves cannot undergo much transport before becoming so degraded that they are no longer useful, and so when found reasonably well-preserved tend to record conditions close to their depositional locations in basin lowlands (Ferguson, 1985; Spicer & Wolfe, 1987). As such, palaeoelevations derived from leaves complement those derived from stable isotope fractionation (Spicer, *et al.*, 2020c). By contrast, the long-distance transport and re-working potential of palynomorphs make them problematic for quantitative palaeoaltimetry and may give an elevation signal that reflects the range of altitudes occupied by their source plants (Su *et al.*, 2019) and not of where they were deposited. Ideally both stable isotopes and plant megafossils should be used in tandem to reconstruct past landscapes (Spicer *et al.*, 2020c).

Both NLR and CLAMP analyses have been used to quantify past land surface heights from plant fossils (e.g. Axelrod, 1981, 1997; Axelrod & Bailey 1976; Forest *et al.*, 1999; Gregory, 1994; Gregory & Chase, 1992; Gregory & McIntosh, 1996; Khan *et al.*, 2014; Song *et al.*, 2020; Spicer *et al.*, 2003; Su *et al.*, 2019, 2020). Both approaches are capable of returning mean annual temperatures and thermal extremes (cold and warm monthly or seasonal temperatures) and so both can be used to estimate surface height based on thermal lapse rates, but there are several kinds of thermal lapse rates, each with its own characteristics.

### Thermal lapse rates

Thermal lapse rates describe changes in temperature with changing elevation. In general (with the exception of a temperature inversion) temperature declines with increasing height and can be expressed as:

$$\Gamma = -dT/dz$$

where  $\Gamma$  is the lapse rate,  $dT$  is the change in temperature, and  $dz$  is the change in height.

Lapse rates can be measured in a column of static (non-convecting) free air (environmental lapse rates— $\Gamma_e$ ), or close to the land surface (terrestrial lapse rates— $\Gamma_t$ ) where the thermodynamics of land surface–atmosphere interactions complicate general trends. Moreover, they can be defined in terms of temperatures measured by either dry bulb or wet bulb thermometers, and not just annual mean temperatures, but also seasonal or even monthly means (Farnsworth *et al.*, 2021).

Many previous palaeoaltimetric estimates have used modern global mean environmental lapse rates based on

annual averages. This is wholly inappropriate for several reasons: 1) plants do not live suspended in a column of free air, but grow attached to the land surface, 2) mean annual temperatures mask a wide range of spatiotemporal thermal regimes where plant growth is constrained not by the mean annual conditions, but by winter cold and/or summer heat, and 3) thermal lapse rates change over time, particularly as a function of atmospheric composition, especially moisture content (Meyer, 1992, 2007; Wolfe, 1992; Spicer, 2018; Farnsworth *et al.*, 2021).

Although modern global mean free air lapse rates ( $\Gamma_e$ ) might be readily available, easy to use, and will appear quantitative because they generate a number constrained by real-world observations, the numbers they give are likely to bear little relationship to past reality, meaning a lot of height estimates in existing literature are meaningless or misleading. This is because both plant and isotope proxies represent conditions close to or just below the land/river/lake/soil surface relevant to the thermal proxy. A better approach is to use terrestrial lapse rates ( $\Gamma_t$ ) because they reflect more closely the conditions captured by the proxy. Unfortunately, terrestrial lapse rates are very different to environmental lapse rates because close to the ground surface characteristics (roughness, albedo, moisture availability, thermal capacity etc.), turbulence and convective processes alter the thermal regime from what it would be in a column of free air. Consequently, terrestrial lapse rates vary not only through time, but are also highly dependent on local landscape properties, and can even become negative (temperature increases with altitude) in basins experiencing temperature inversions on a regular basis (Wolfe, 1992). When local topography is what we are trying to determine this is problematic.

To overcome this potentially circular problem we need to combine proxy data with coupled ocean–atmosphere numerical climate modelling that incorporates our current understanding of the behaviour of the integrated (ocean, atmosphere, biosphere, cryosphere) climate system. An example of how this can be done is given in Su *et al.* (2019) where the frost sensitivity of natural palm populations (Reichgelt *et al.*, 2018), combined with a range of possible modelled topographies (sensitivity analysis) and past boundary conditions, were used to determine a maximum height and topographic configuration that could have supported palm growth. In this case a palaeoclimate model-derived local cold month mean terrestrial lapse rate was used. This kind approach now needs to be further refined using higher spatial resolution climate modelling in an iterative way to converge on more accurate depictions of past landscapes.

Recently, climate modelling has also been used to explore the different characteristics of thermal lapse rates. Within 'model world' several topographic scenarios for the Tibetan region were used to test the ability of different thermal lapse rate formulations to reconstruct those hypothetical landscapes. The modern pre-industrial world was compared to the Eocene

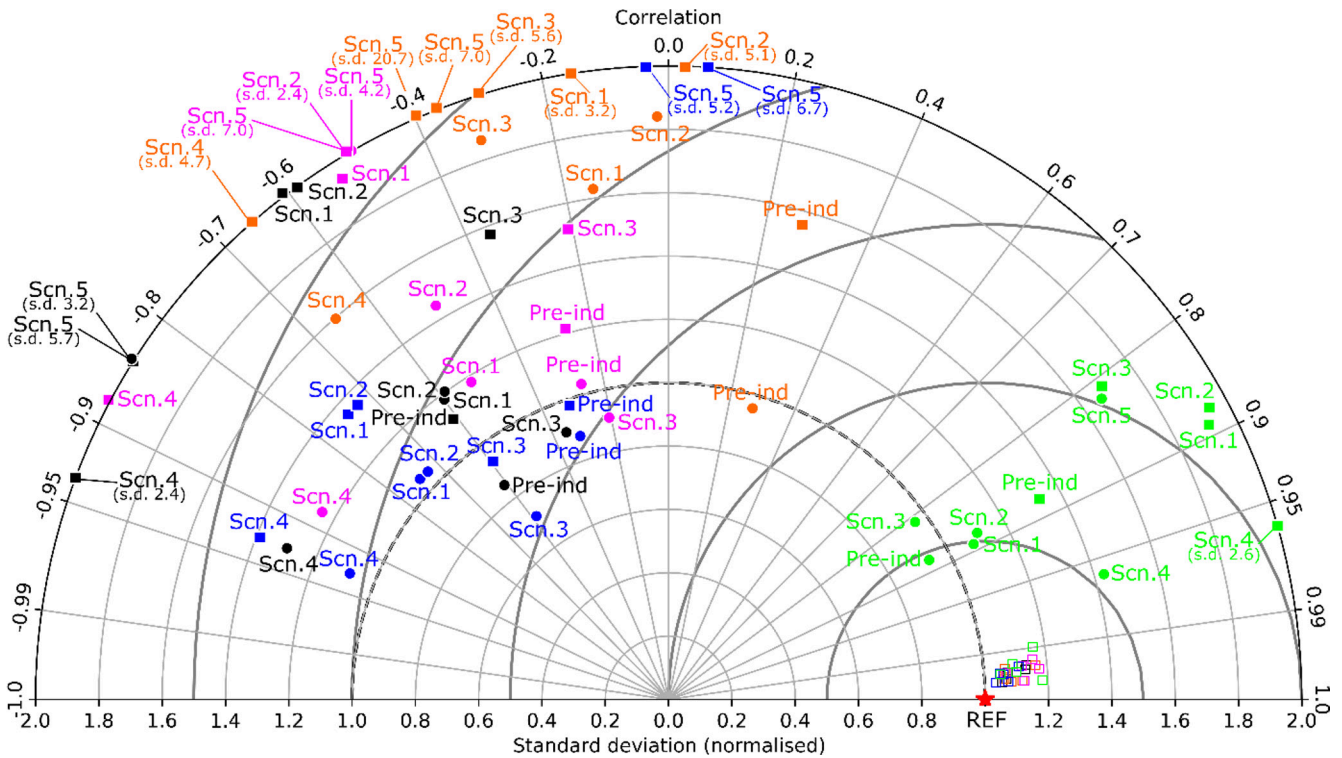


Fig. 6—Taylor diagram depicting the skill within a numerical climate model of using annual (black) and seasonal (DJF (Pink), MAM (Green), JJA (Orange), SON (Blue)) global mean free air environmental ( $T_e$ ) (circle symbol) and terrestrial lapse rates ( $T_l$ ) (square symbol) to reconstruct the prescribed Tibetan topography (>2000m) for each simulation scenario (scn, Pre-industrial, and five Lutetian topography sensitivity studies). Temperatures were those representing 1.5m surface dry bulb temperatures (closed symbols) and wet bulb temperatures (open symbols). Each reconstruction is normalised relative to the prescribed reference topography (star symbol). Points positioned closer to the red star symbol depict greater predictive skill. In this case wet bulb  $T_l$  far outperformed dry bulb  $T_l$  or  $T_e$  for reconstructing palaeoaltimetry. Modified from Farnsworth *et al.* (2021).

(Lutetian) and these experiments showed that the only thermal lapse rates capable of reconstructing past landscapes as prescribed in the model were terrestrial lapse rates based on wet bulb temperatures (Fig. 6). All other lapse rates performed poorly because moisture, as well as temperature, varies with height (Farnsworth *et al.*, 2021). This means that almost all previous palaeoelevation estimates based on thermal lapse rates now need to be re-evaluated. However, wet bulb thermal lapse rates offer great potential if multiple proxies can be recalibrated to deliver wet bulb temperatures. CLAMP seems to code well for wet bulb temperatures (Fig. 7) and recalibration of NLR approaches should be relatively trivial. This approach now needs to be properly field-tested.

**Moist Static Energy, moist enthalpy and energy conservation**

At the time of writing only CLAMP has been calibrated to return moist enthalpy which, using the principle of conservation of energy, can also be used to derive surface height estimates (Forest *et al.*, 1995, 1999). Moist enthalpy is less affected by topography and atmospheric composition, combines both temperature and moisture, and tends to be more

zonal (primarily varying with latitude) than lapse rates (Forest *et al.*, 1995). It is therefore more straightforward to use.

When a parcel of air rises up through the atmosphere it gains potential energy and expands, and as it does so it cools and its humidity rises, but the overall combination of these properties remains the same to comprise what is termed 'moist static energy'. The term 'static' indicates that kinetic energy is ignored which, except during a hurricane, is negligible. The temperature and moisture content comprise what is known as moist enthalpy ( $H$ ), while potential energy is the product of height ( $Z$ ) times the gravitational constant ( $g$ ). Because moist static energy is conserved as the air parcel moves through the atmosphere any difference in enthalpy between the start of an air parcel upslope trajectory and a given point along that trajectory, divided by the gravitational constant will give the height difference ( $\Delta Z$ ) between those two points.

$$\Delta Z = (H_{low} - H_{high})/g$$

Fortunately, moist enthalpy is coded well in leaf form (Forest *et al.*, 1995), and so can be derived from a fossil assemblage using CLAMP. For a commonly used CLAMP calibration for Asia (PhysgAsia2) the statistical uncertainty

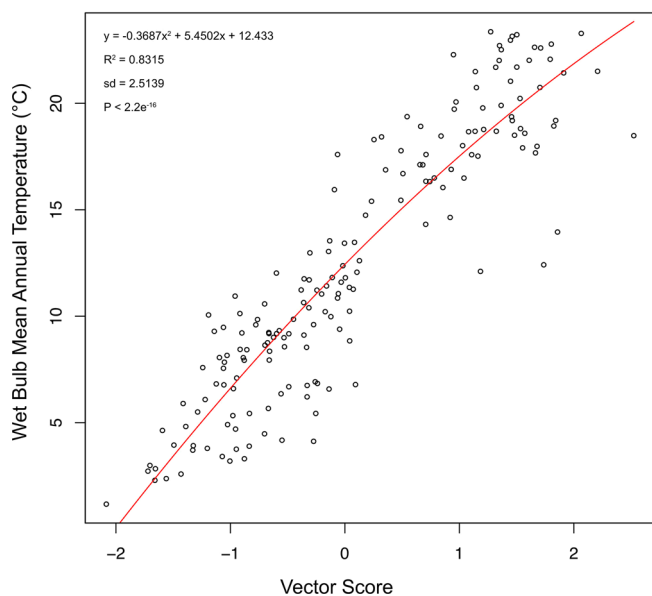


Fig. 7—CLAMP wet bulb mean annual temperature regression for the PhysgASia2 calibration showing the strong correlation of leaf traits with wet bulb temperature. The black open circles represent modern vegetation samples positioned based on their leaf trait spectra. The vector score represents the relative position along a vector describing the trend in wet bulb mean annual temperature in four-dimensional physiognomic space. For a detailed explanation of CLAMP regressions see Spicer *et al.* (2020).

in deriving moist enthalpy using WorldClim2 climate data at  $\sim 1\text{km}^2$  spatial resolution (Fick & Hijmans, 2017) is  $800\text{ m}$  ( $1\sigma$ ) (Spicer *et al.*, 2020d). All the preceding techniques have been applied to quantifying landscape evolution across the Tibetan Plateau, the Himalaya and the Hengduan Mountains region (THH).

## QUANTIFYING THE PALAEO TOPOGRAPHY OF THE THH REGION

Here we will define the THH region as encompassing what is today's Tibetan Plateau, the Hengduan Mountains and the Himalaya (Fig. 4). The southern boundary of the plateau is marked by the Yarlung–Tsangpo Suture Zone (YTSZ) (Figs 4 and 8) so the Himalaya are part of the Indian Plate and distinct from the plateau. To the north of the YTSZ is the Lhasa terrane, a piece of Gondwana that accreted to Asia in the Late Jurassic to Early Cretaceous (Kapp & DeCelles, 2019). The northern boundary of the Lhasa terrane is marked by the Bangong (or Banggong)–Nujiang Suture Zone (BNSZ), north of which is the Qiangtang terrane, another piece of Gondwana that joined to the Songpan–Ganzi terrane in the Triassic. Collectively the Lhasa, Qiangtang and Songpan–Ganzi terranes, together with other smaller continental blocks, comprise the modern Tibetan Plateau.

The Tibetan Plateau is characterised by its generally low relief surface extending over an area approximately  $2,500,000$

$\text{km}^2$ , most of which is higher than  $4.5\text{ km}$ . However, it was not always a plateau so the term 'Tibetan Plateau' can only be applied to describe its present condition. Careless use of the term 'plateau' before a low relief surface was formed confounds rigorous discussions of landscape development and its consequences (Spicer *et al.*, 2020b). The Hengduan Mountains have no clear boundary with the plateau proper, but ramp down south–eastwards into Yunnan.

## The THH Region in the Cretaceous

The Gangdese Mountains are located along the length of the southern margin of the Lhasa terrane (Fig. 4), and before the arrival of India and the rise of the Himalaya they formed the southernmost uplands of Eurasia bordering the Neotethys Ocean (Ding *et al.*, 2014). The height of this Andean-type magmatic arc in the Late Cretaceous is not well quantified, but could have been  $2\text{ km}$ , or slightly higher, due to the subduction of Neothethyan Ocean floor prior to the arrival of the Indian Plate. Until the late Early Cretaceous a shallow marine remnant of the meso–Tethys Ocean extended northwards from the rising Gangdese across the BNSZ to uplands on the Qiangtang terrane (Kapp & DeCelles, 2019). This Qiangtang upland is variously referred to as the Tanghula (Tanggula) range, or the Central Watershed mountains. These shallow marine sediments ceased to be deposited at around  $105\text{ Ma}$  and this local regression appears to have been diachronous east to west (Kapp & DeCelles, 2019). The Late Cretaceous climate across much of the region seems to have been arid to semi-arid (Farnsworth *et al.*, 2019 and references therein) and this aridity extended into the early Paleocene (Fig. 10).

## The Tibetan Region in the Paleogene

The first quantitative surface height measurement of the Gangdese arc is for the early Eocene ( $\sim 56\text{ Ma}$ ) in the form of an estimate of  $\sim 4.5\text{ km}$  based on oxygen isotopes preserved in the Linzhou Basin (Ding *et al.*, 2014). Because of the fractionation bias towards mountain ridges this may well reflect the then crest height of the range. By the mid Miocene to Pliocene the height of the Namling–Oiyug and Zanda basins within the Gangdese range increased to  $\sim 5\text{ km}$  (Currie *et al.*, 2016; Huntington *et al.*, 2015; Khan *et al.*, 2014; Polissar *et al.*, 2009; Saylor *et al.*, 2009), after when these basin floors appear to have subsided, perhaps by as much as  $1\text{ km}$  (Huntington *et al.*, 2015; Khan *et al.*, 2014; Saylor *et al.*, 2009). This suggests that the Gangdese persisted throughout the Paleogene as a significant highland, which must have had profound effects on atmospheric circulation as is evident in modelled wind patterns (Fig. 9).

The centre of what is now the Tibetan Plateau evidently remained low throughout the Paleocene. This is suggested by low elevation peneplanation across the northern part of the Lhasa terrane (Hetzl *et al.*, 2011), and the Gerze Basin,  $\sim 350$



Fig. 8—View in central southern Tibet from the northern edge of the Indian Plate westwards along the Yarlung–Tsangpo Suture marked by the Tsangpo (Brahmaputra) River, with the remnant Gandgese Mountains to the right of the river in the distance.

km west of the Nima Basin (Fig. 4) along the BNSZ, remained near sea level until the late Eocene (Wei *et al.*, 2016). As early as the middle Eocene (~47–45 Ma), however, the Bangor Basin, also along the BNSZ, had risen to  $\sim 1.5 \pm 0.9$  km (Su *et al.*, 2020). The Bangor Basin surface height estimate was based on a moist enthalpy CLAMP analysis of the extremely diverse 'Shangri-La' subtropical Jianglang fossil flora, which

currently is known to comprise ~70 different plant taxa. This flora exhibits strong phytogeographical similarities to middle Eocene floras in North America (Green River) and Europe (Messel), but with only a few taxa in common with India. This paucity of Gondwanan elements suggests the Gandgese may have presented a strong barrier to plant migration from India into central Tibet.

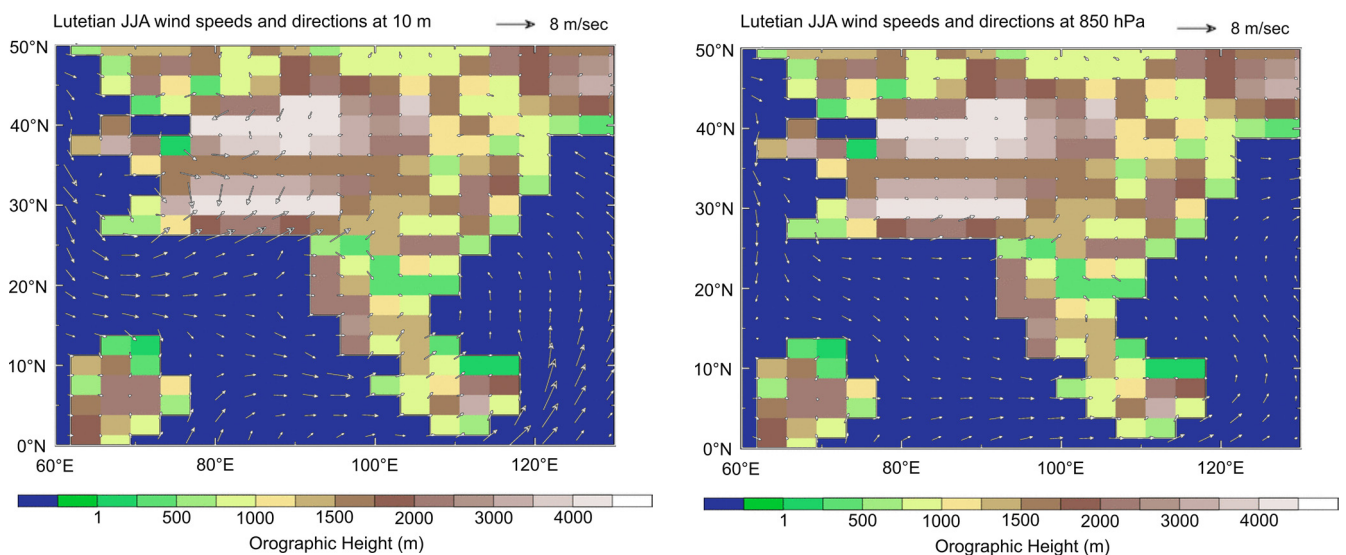


Fig. 9—Middle Eocene (Lutetian; ~44 Ma.) climate model simulations under 1120 ppm pCO<sub>2</sub> 10 m surface (left panel) and 850 mb (right panel) wind speed (vectors; m/s) and orography (contoured; m) in June–August. Note that while there is some west to east airflow within the Tibet central valley (~35°N) very little surface of high-altitude winds (and thus moisture) enters directly from the Paratethys. There are, however, significant surface winds moving northwards from the Neotethys up the southern slopes of the Gandgese (~30°N).

The Jianglang plant composition is typical of a seasonal, humid, sub-tropical ecosystem and this is confirmed by the CLAMP analysis, which points to a warm climate (MAT  $18.9 \pm 2.4^\circ\text{C}$ ) where frosts were rare (CMMT  $\sim 7.4^\circ\text{C}$ ), but overall annual rainfall was seemingly high ( $\sim 2\text{ m}$ ) with marked wet-dry seasonality (Summer VPD  $14.7 \pm 3.5\text{ hPa}$ , winter VPD  $5.6 \pm 1.5\text{ hPa}$ ). The Jianglang leaf physiognomic spectrum is similar to that typical of the EAM over southern China and the SAM, so indicates a distinctly monsoonal system (Su *et al.*, 2020). Note though that this monsoon was not necessarily the same as the modern ones.

This monsoon-affected lowland seems to have persisted until sometime in the late Eocene to early Oligocene. Dating of the critical Dayu section in the Lunpola Basin (Rowley & Currie, 2006; Su *et al.*, 2019; Liu, 2018; Fang *et al.*, 2020) remains unresolved in the upper part of the section because of significant depositional gaps formed by fluvial erosion and soil forming intervals, but a newly discovered (Fang *et al.*, 2020) primary tuff (ash fall) now constrains the age of the sub-tropical Dayu biota (Wu *et al.*, 2017) containing palms (Su *et al.*, 2019) to  $\sim 39\text{ Ma}$  instead of  $25\text{ Ma}$  as assumed previously. A re-analysis using a climate model with Bartonian boundary conditions only raises the maximum survivable elevation for the palms from the originally published  $2.3\text{ km}$  (Su *et al.*, 2019) to  $2.85\text{ km}$ , far below the  $\sim 4.5\text{ km}$  elevation estimated using oxygen isotopes (Rowley & Currie, 2006).

Although the uncertainties in the Jianglang and Dayu height estimates overlap, it is possible that this part of central Tibet along the BNSZ was beginning to rise in the middle Eocene, but when it reached its near present elevation of  $\sim 4.5\text{ km}$ , as suggested by the stable isotope work of Rowley and Curry (2006), remains unclear. This is because the upper Niubao Formation bearing the palaeosol nodules that formed part of the Rowley & Curry (2006) analyses is reported to have within it 'tuffites' (reworked volcanic ashes) indicating a minimum age of  $23.3 \pm 0.3\text{ Ma}$  (Fang *et al.*, 2020) and thus age-equivalent to a similar tuff (bentonite) that occurs within the lower Dingqing Formation (He *et al.*, 2012) that supposedly overlays the Niubao. However, other sampling of several tuffites within the upper Niubao has failed to find zircons younger than  $37\text{ Ma}$ , with the youngest possible age of the upper Niubao being constrained by a  $29\text{ Ma}$  tuff at near the base of the overlying Dingqing Formation (Liu *et al.*, 2018).

The magnetostratigraphy proposed by Fang *et al.* (2020) does not adequately constrain the age of the Rowley and Currie (2006) Dayu samples because even if the report of the  $23.3\text{ Ma}$  tuffite is not an error, it only provides a minimum age because it is reworked and the upper parts of the section contain numerous erosion surfaces and depositional hiatuses (Liu, 2018) not recognised by Fang *et al.* (2020). We do not yet know if these hiatuses are regional or local, or if the contact between the upper Niubao and overlying Dingqing Formation is diachronous, but breaks in sedimentation and a static surface persisting long enough to develop palaeosols

represent unknown amounts of time not represented by sediment accumulation, and is therefore 'missing'. A clue as to when significant uplift had taken place is offered by a switch from a humid to a drier environment at  $\sim 23.5\text{ Ma}$  recorded in the Dingqing Formation exposed in the Lunpori and Chebuli sections, as well as in the Wang-1 borehole (Ma *et al.*, 2017), all within the Lunpola Basin and just above a bentonite dated at  $23.6\text{ Ma}$ . This suggests that by the start of the Neogene a high semi-arid landscape environment similar to that of today existed in central Tibet.

### Eastern Tibet and the Hengduan Mountains

This story of late Paleogene gains in surface height also applies to eastern Tibet where uplift of the Hengduan Mountains seems to have begun even earlier than in central Tibet. Climate model validated oxygen isotope palaeoaltimetry within the Gonjo Basin (Fig. 4) shows a rise from  $\sim 700\text{ m}$  at  $54\text{--}50\text{ Ma}$  (early Eocene) to a near-present elevation of  $3,800\text{ m}$  by  $40\text{ Ma}$  (middle Eocene) (Xiong *et al.*, 2020), while  $\sim 100\text{ km}$  to the southeast the Markam Basin had achieved its present elevation of  $3.9\text{ km}$  by the earliest Oligocene, and likely was rising rapidly in the latest Eocene (Su *et al.*, 2018). Again, CLAMP-derived moist enthalpy was used to obtain this elevation estimate and other CLAMP climate metrics suggest only a modest fall in MAT in this elevated part of eastern Tibet across the Eocene-Oligocene (E-O) boundary. This cooling from  $17.8 \pm 2.3^\circ\text{C}$  MAT in the latest Eocene to  $16.4 \pm 2.3^\circ\text{C}$  in the earliest Oligocene was accompanied by a distinct drying of the dry season to increase rainfall seasonality, but not to a degree of seasonality that could be considered monsoonal. Nevertheless, this climate shift is associated with a marked change in the young Hengduan Mountain vegetation from one typical of subtropical to warm temperate mixed evergreen and deciduous communities in the latest Eocene to a more temperate type with smaller leaves in the earliest Oligocene (Su *et al.*, 2018).

It is becoming clear through recent radiometric re-dating of several basins in Yunnan (Gorbet *et al.*, 2017; Linnemann *et al.*, 2018; Li *et al.*, 2020; Tian *et al.*, 2021) that many highly diverse palaeofloras previously considered as mid to late Miocene in age are in fact early Oligocene, and that major tectonic restructuring was taking place in Yunnan in the late Eocene to Oligocene. The palaeoelevation of these basins remains controversial (Li *et al.*, 2015; Hoke *et al.*, 2014; Hoke, 2018), but it seems that a steep south-to-north elevational gradient of  $\sim 4.5 \pm 1\text{ km}$  across Yunnan, similar to the  $3.4 \pm 1\text{ km}$  seen today, was established by the late Eocene (Hoke, 2018). This is also the time ( $\sim 35\text{ Ma}$ ) when a major re-organization of regional drainages took place (Clift *et al.*, 2020). Based on rock cooling rates (possibly indicative of uplift) it seems that parts of the Hengduan uplands may have been rising in the Late Cretaceous (Liu-Zeng *et al.*, 2018), but overall the Hengduan Mountains were mainly a Paleogene

construct such that by the early Oligocene much of the present elevation had been attained. Note, however, that cooling rates may be enhanced by unroofing (erosion) driven by increased weathering and rainfall, and so do not necessarily translate into uplift. Major drainages (e.g. those of the Red River and the Yangtze) were established during the Eocene/Oligocene (Clift *et al.*, 2020) tectonic restructuring, but it is also likely that topographic relief (landscape dissection) was enhanced through river incision in the Miocene, possibly through increased monsoon-related rainfall (Nie *et al.*, 2018), and this is reflected in exhumation rates (Wang *et al.*, 2012).

Several Yunnan basins previously regarded as Miocene but now re-dated to early Oligocene preserve highly diverse fossil plant assemblages with many of the identified taxa being closely allied to extant forms. This was the main reason why these assemblages were previously regarded as Miocene. The most recent work of this kind is that by Tian *et al.* (2021) who re-dated the Wenshan flora to the early Oligocene (30–32 Ma) and so roughly contemporaneous with that of the Lühe Basin (Linnemann *et al.*, 2018; Li *et al.*, 2020). The Wenshan flora is exceptionally diverse, comprising more than 200 species of predominantly tropical to subtropical taxa with some elements typical of those growing on modern limestone karst landscapes. The overall composition displays affinities to the modern Sino–Japanese flora east of the 'Tanaka' line (Tanaka, 1954; Wu *et al.*, 2006) that runs through Yunnan, and is quite different to the Tibet–Himalaya flora that exists further west and is seen in the Lühe floral composition (Tang *et al.*, 2020).

Normally our understanding of past vegetation is derived from fossil assemblages, but some communities are never, or rarely, preserved because they grow on mountain sides away from depositional environments, and this applies *in extremis* to alpine plant assemblages. However, by using molecular phylogenetic analysis of extant alpine plants it has been possible to document major diversification events within the THH (Ding *et al.*, 2020). Time-scaled molecular phylogenies suggest there was a pulse of *in situ* speciation in the Hengduan Mountains at 27 to 24 Ma (late Oligocene) followed by one in the Himalaya beginning at 19 to 17 Ma (early Miocene), peaking in the middle Miocene. *In situ* speciation dominates in the Hengduan Mountains to the present day, exceeding rates of colonization. Diversification of alpine plants across the Tibetan Plateau region was, by contrast, dominated by colonization throughout the Miocene and only in the last 5 Ma have rates of *in situ* speciation started to rise (Ding *et al.*, 2020).

These findings are congruent with the geological evolution of the region and provide independent validation of the palaeoaltimetry. The Hengduan Mountains had achieved high enough elevations in the Oligocene that, despite an overall warmer-than-present global climate, afforded sufficient land surface above the then tree line to favour alpine plant speciation. The subsequent *in situ* diversification in the Himalaya matches the timing of their rise to at least 4.5

km by the mid Miocene (Ding *et al.*, 2017; Xu *et al.*, 2018), although it is possible that some of the diversification also took place in the more ancient Gangdese Arc and that those plants migrated to the Himalaya or went extinct (and so not detectable in surviving taxa) due to subsequent drying as the Himalayan rain shadow developed after the mid Miocene. The low rates of *in situ* speciation among plateau alpine taxa may be due to large parts of what is now the plateau being at elevations below the tree line throughout much of the Paleogene and early Neogene, only becoming available to alpine taxa as global cooling progressed in the Pliocene to recent, after the present plateau became fully formed in the Neogene.

### The evolution of Himalayan vegetation under a monsoon climate

The rise of the Himalaya was accompanied by the development of the Himalayan Foredeep Basin that began accumulating sediments about 50 million years ago. These sediments, now partly uplifted by the ongoing southward advance of Himalayan uplift (Ding *et al.*, 2017) are best exposed in the Siwalik succession. The Siwaliks are separated from the Lesser Himalaya by the Main Boundary Thrust and from the Indo–Gangetic plains by the Main Frontal Thrust. Dissection by numerous rivers draining the Himalaya exposes the uplifted foreland sediments mostly comprising shale, siltstones, mudstones, sandstones, palaeosols and conglomerates that record the history of Himalayan erosion and monsoon development (e.g. Clift, 2017; Clift *et al.*, 2008; Coutand *et al.*, 2014, 2016; Jain *et al.*, 2009). Recent re-analyses of contained floras (Bhatia *et al.*, 2021a; Hazra *et al.*, 2020; Khan *et al.*, 2014, 2019), which have been known and studied for some while (Antal & Awasthi, 1993; Antal & Prasad, 1996a, b; 1997, 1998; Awasthi, 1992; Banerjee, 1996; Banerjee & Dasgupta, 1984, 1996; Cautley, 1835; Khan & Bera, 2014a, b; Khan *et al.*, 2011, 2014, 2015, 2016, 2017a, b; Prasad, 1994a–c; Prasad & Pandey, 2008; Prasad & Tripathi, 2000) point to monsoon conditions having existed throughout the Neogene. What is not yet clear is when today's pronounced west to east increasing precipitation gradient developed along the Himalayan front, and what vegetation changes accompanied the drying in the west.

### Monsoons over Southern China and the East Asia Monsoon

The history of the East Asia Monsoon (EAM) is complex, with some authors even questioning if it should be considered a monsoon at all (Molnar *et al.*, 2010). The most recent comprehensive modelling study is that of Farnsworth *et al.* (2019) who explored the gross effects of palaeogeography and CO<sub>2</sub> changes from the Early Cretaceous to present (Fig. 10), and compared the model precipitation simulations with proxy data. They found that monsoonal conditions prevailed

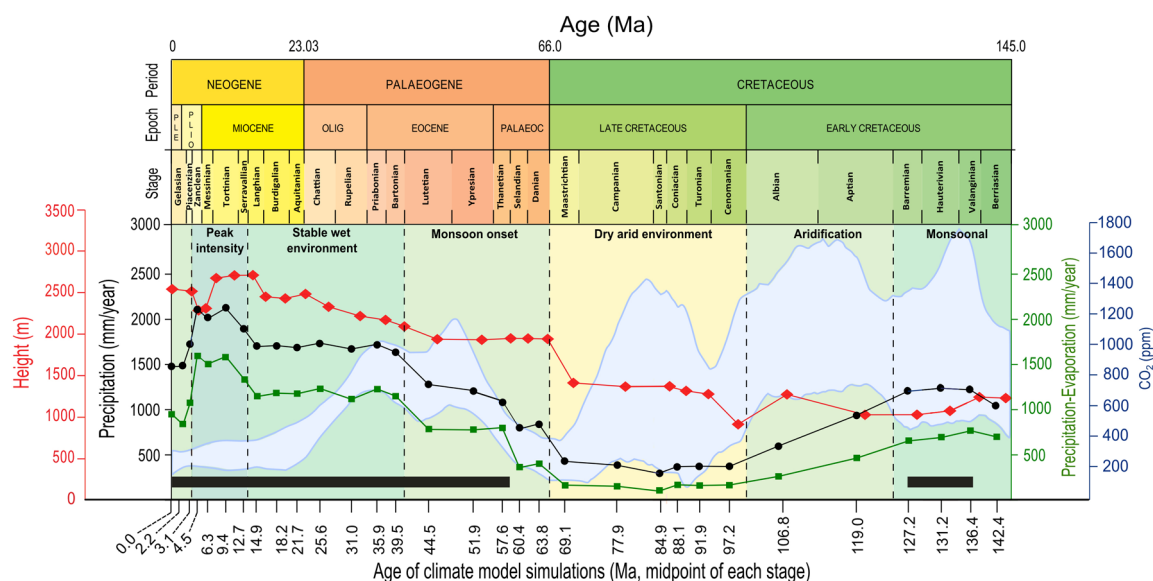


Fig. 10—Palaeoclimate modelling of monsoons over eastern Asia. Each point represents precipitation (black solid circles) and precipitation–evaporation (green filled squares) simulations produced by numerical climate models configured for boundary conditions at each stage from the Berremian to present. Mean heights for the THH used in each simulation is indicated by red diamonds. Light blue band indicates atmospheric CO<sub>2</sub> estimates from proxies. Modified from Farnsworth *et al.* (2019).

between the Valanginian to Barremian, after which there was progressive drying until the middle Cretaceous. Arid conditions persisted across southern Asia until near the end of the Paleocene when monsoon conditions returned and lasted until the present. Regional precipitation increased steadily throughout the Cenozoic, reaching peak intensity in the late Miocene to Pliocene. Eocene to Oligocene plant fossil assemblages from Hainan Island and the Maomin Basin in southern China tend to confirm the presence of a weak, but intensifying, monsoon characterised by increasing rainfall seasonality (Spicer *et al.*, 2017), but interpretations are complicated by not being able to quantify the palaeoelevation of these sites due to the lack of a nearby demonstrably sea level fossil floras.

The EAM is not just a modified ITCZ monsoon because the poleward summer migration of the ITCZ is enhanced by the development of the summer Siberian low and this amplification is protected by the deflection of the westerlies by the elevated THH. In the winter the development of the extremely cold Siberian high–pressure system drives cold dry air south–eastwards over northern China.

Over the years there have been numerous attempts to try and understand when the EAM became established, but like other monsoon studies these attempts have suffered from poor characterisation as to what constitutes the EAM. Atmospheric circulation changes through time and there is a lack of suitable proxies to capture unique EAM signatures. One palaeobotanical contribution that stands out and which focusses on the unique expansion of the EAM into northern China is that by Quan *et al.* (2011) who argued for a late middle Eocene intensification. This is interesting because not

only does it seem to tally with the modelling of Farnsworth *et al.* (2019) but it points to a time when substantial changes were taking place in the topography of the THH, which is so critical in deflecting the westerlies.

The Quan *et al.* (2011) work utilised the Co–existence NLR Approach, and a recent analysis (Xie *et al.*, 2021) that used the same technique concluded that central Tibet experienced a monsoonal warm humid climate in the late Oligocene. Fluctuations in seasonal precipitation varied in line with what appear to be orbital cycles, but that the monsoon type (SAM or EAM) could not be differentiated. Orbital variations in climate are, of course, inevitable (e.g. Leuschner & Sirocko, 2003), which in turn drive vegetation changes (Claussen *et al.*, 2006; Tuenter *et al.*, 2006) used as the proxy, but the work lacks detail regarding the dating model for the section, and they use an out of date concept for the topographic development of the THH. Much more rigor is required if we are to properly understand the evolution of monsoon characteristics over Asia.

In another paper (Wang *et al.*, 2021), which shares many of the authors of Xie *et al.* (2021), the Coexistence Approach was applied to 75 Miocene plant (pollen) assemblages across China and concluded that the latitudinal thermal gradient across China was shallower than today, but not as shallow as in the Eocene, and that the 'Asian monsoon' was still in its infancy in the Miocene. Moreover, it was inferred there was no evidence of a rapid 'uplift of the Tibetan Plateau' or other high topography in the Miocene. This of course ignores spatial 'smearing' produced by long distance transport of palynomorphs. Moreover, this work does not cite any of the recent literature we have considered here regarding the

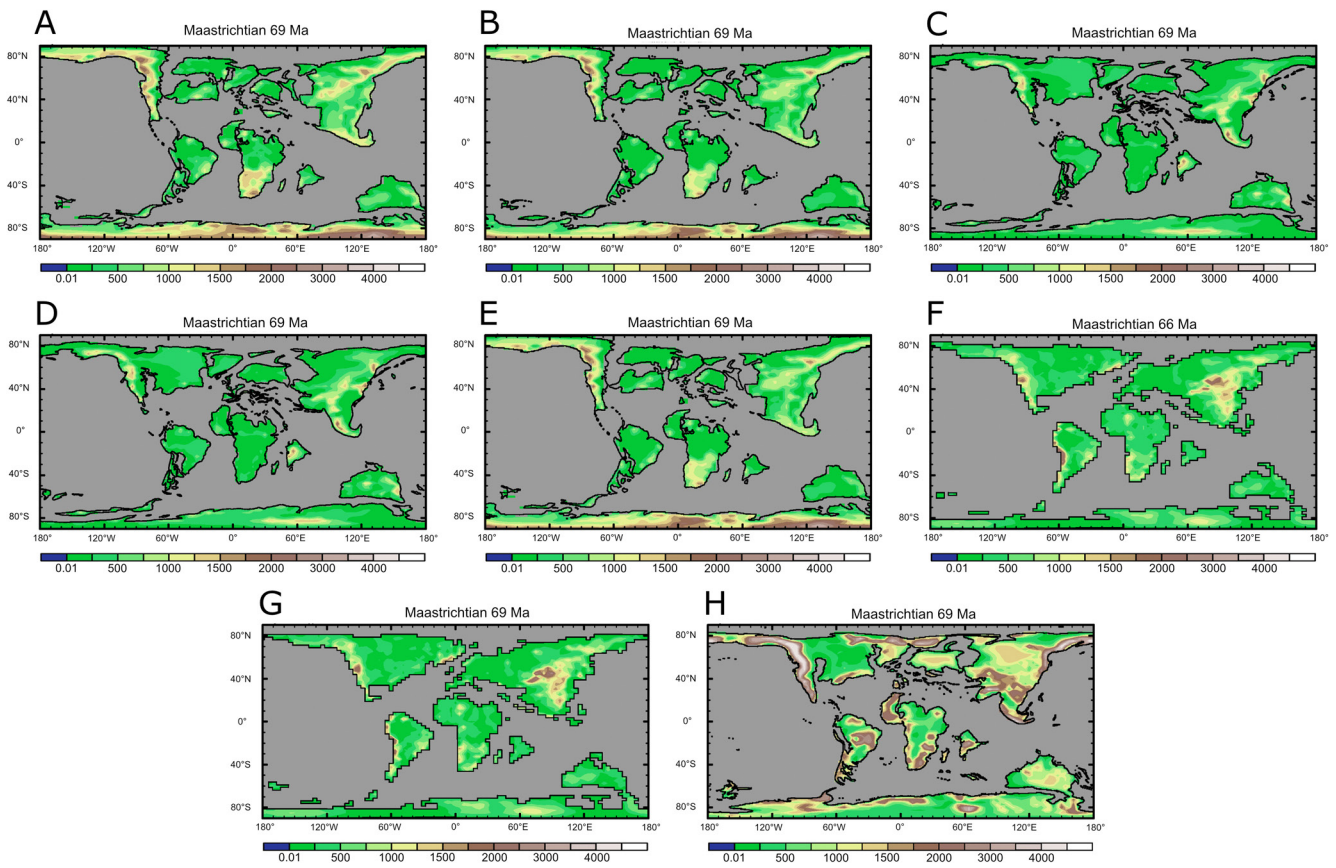


Fig. 11— Different Palaeogeographic reconstructions for the Maastrichtian (~69 Ma). (A) Markwick Palaeogeography (Markwick & Valdes, 2004), (B) similar to panel A but with a revised methodology for converting to GCM grid, (C) Robertson Plc. (2016), (D) Robertson Plc. (2017), (E) As panel A, but with Arctic Ocean gateways opened, (F) Scotese, Late Maastrichtian (~66 Ma), (G) Scotese, Early Maastrichtian (~69 Ma), Getech Plc. (Farnsworth, *et al.* 2019). Surface heights are given in metres.

orogeny of the Tibetan region, nor does it take into account any Miocene topographic variability across the rest of China at that time. This highlights the need to have a broad perspective covering publications across a wide range of disciplines to make sense of the relationships between orography, climate and biodiversity in order to interpret the fossil record of the region.

## POSSIBLE WAYS FORWARD

### Proxy Improvements

Currently the CLAMP modern vegetation training data are devoid of leaf trait spectra from vegetation adapted to cool climates dominated by the SAM. This could be rectified by collecting from modern elevations in the Himalaya up to the tree line. When this is done it may be possible to distinguish SAM traits from those developed in south China vegetation exposed to the EAM, but this cannot be guaranteed. That is the nature of research.

The promise evident in using wet bulb terrestrial thermal lapse rates instead of those based on dry bulb temperatures

now needs to be applied more widely by recalibrating NLR methods to yield wet bulb temperatures. This will not overcome the problems of spatial and temporal smearing inherent on any pollen-/spore-based climate interpretations, but it may help provide reliable baseline data if we use only the tolerances of the most thermophilic taxa to obtain minimum elevations.

The use of moist enthalpy to obtain palaeoelevations appears extremely robust but there are still some uncertainties about spatial averaging of the elevation estimates it returns. At the spatial scale of conventional climate models (e.g. the grid cell size in Fig. 9) moist enthalpy is able to reproduce well the model prescribed topography, but over highly dissected landscapes it does not perform as well. More research is required to fully understand what the numbers it returns for ancient surface heights really represent in terms of spatial scale.

### Modelling

Palaeoclimate modelling allows us to interpolate between spatially and temporally incomplete proxy data, but to be

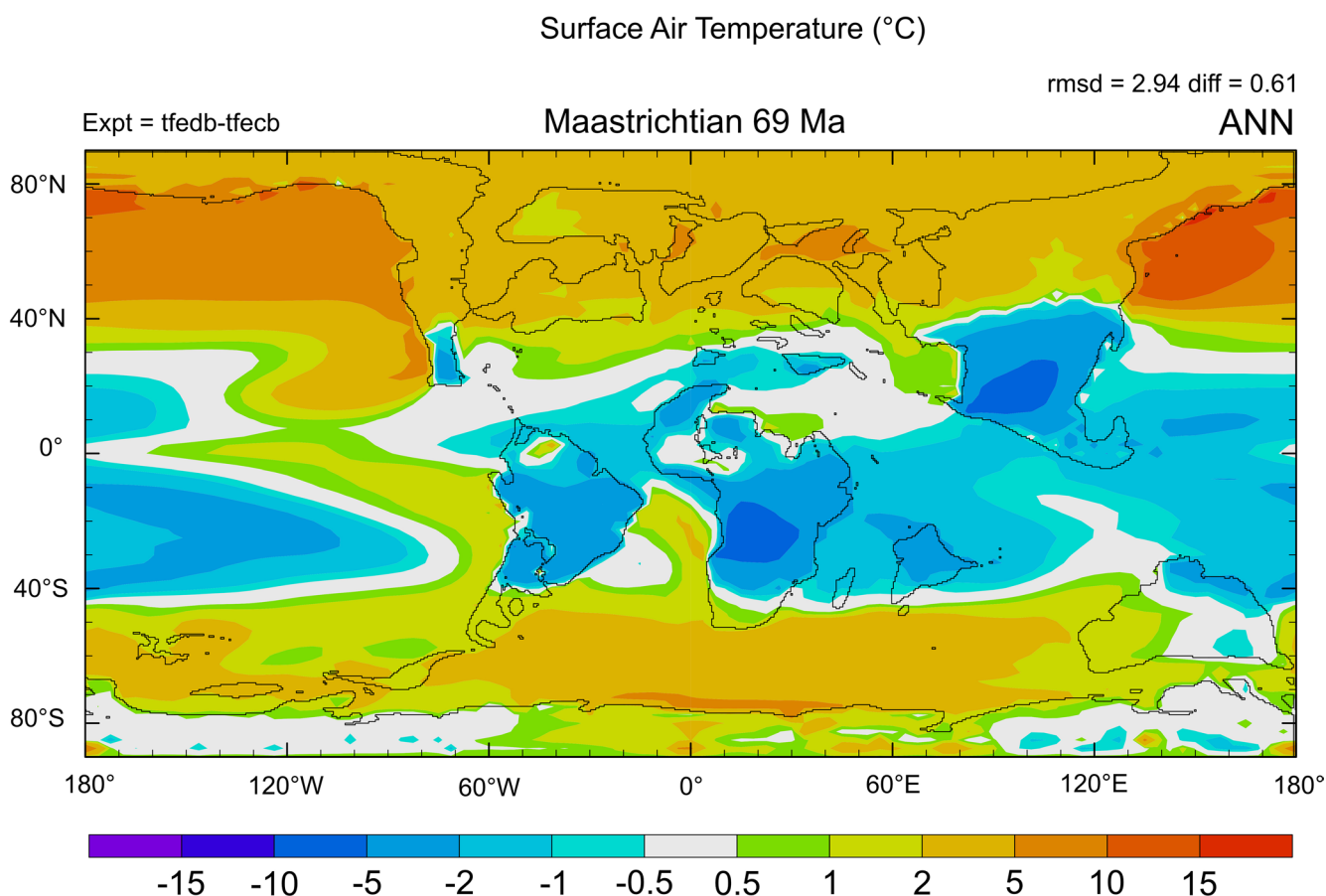


Fig. 12—1.5 m surface temperature anomaly for the Robertson's Plc. palaeogeography (see Figure 10 (c)) for the Maastrichtian for a HadCM3L general circulation model simulation using a new set of model parameterisations. This shows the difference in mean annual temperature between the old physics and the new. The net effect warms the polar regions and cools the tropics, significantly reducing the pole–equator gradient.

useful the models have to be based on reliable reconstructions of past geography, for which data are inevitably incomplete. Even a cursory look at palaeogeographical reconstructions for a given time slice by different authors (Fig. 11) shows considerable variations, not just in terms of the positions of the individual plates such as India, but critical ocean gateways and topography. Some reconstructions may look attractive, but the details of how they are made are seldom given, and it is difficult to distinguish fact from invention. As palaeogeographic models move to higher spatial resolutions reliable quantification of topography becomes more critical because topography determines both mechanical and thermal atmospheric forcing at local and regional scales.

Using moist enthalpy to determine surface height seems robust and has been cross-validated against isotope techniques where Rayleigh fractionation makes isotope palaeoaltimetry reliable, as in the Namling–Oiyug Basin (Khan *et al.*, 2014; Currie *et al.*, 2016). However, the leaves necessary for using CLAMP are preserved far less often than fruits seeds or pollen. The discovery that wet bulb terrestrial thermal lapse rates offer promise for measuring past surface

heights open new opportunities for recalibrating NLR proxies for palaeoaltimetry. The combination of model-tested palaeoaltimetry proxies and reconstructed topographies, when used iteratively, should greatly improve our ability to better understand the feedbacks and relationships between landscape, climate and biodiversity and allow the development of high spatial resolution models.

Earth system models are also currently limited by their ability to simulate the shallow latitudinal thermal gradients, and the generally equable continental interior climates, that existed in past warmer-than-present climate regimes as indicated by a wide range of proxy data (e.g. Spicer *et al.*, 2008). This phenomenon has been evident for decades (Valdes, 2000), but a way forward has emerged recently through modifying the way that cloud physics is represented in the models. Applications to the Eocene (Zhu *et al.*, 2019) and Maastrichtian (Fig. 12) seem to show great promise in that the polar regions become warmer without over heating the tropics.

This effect is also likely to be relevant over altitudinal gradients, even at low latitudes, and so is relevant to

understanding the interactions between the growth of the modern Tibetan region, monsoons and the Asian biota. The coupling of improved topographic reconstructions with modelling at higher spatial resolutions together with the modified cloud physics should bring about major advances in our understanding of Asian Earth system interactions. Other factors are also proving crucial for the application of numerical models. Often models must simulate many thousands of years (often > 5000, and sometimes even more) to reach full equilibrium in both the atmosphere and deep ocean after time-dependant applied forcing's such as topography, bathymetry, atmospheric carbon dioxide concentrations, ice sheet heights and extents, as well as vegetation (all of which have a host of unconstrained uncertainties) are applied. This is computationally expensive at high spatial resolutions so experiments have to be constructed carefully. From a palaeobotanical perspective the more fossil data we have to constrain topography, evapotranspirational feedbacks, isotope fractionation and albedo, the more reliable palaeoclimate models will be at reconstructing past reality.

**Acknowledgements**—*We are grateful for the invitation to contribute to this special issue. This work was support by an XTBG International Fellowship for Visiting Scientists to R.A.S., and the NSFC–NERC (Natural Environment Research Council of the United Kingdom) joint research program [nos. 41661134049 and NE/P013805/1].*

## REFERENCES

- Acosta RP & Huber M 2020. Competing topographic mechanisms for the summer Indo–Asian monsoon. *Geophysical Research Letters* 47: e2019GL085112.
- Affek H, Bar–Matthews M, Ayalon A, Matthews A & Eiler J 2008. Glacial/interglacial temperature variations in Soreq cave speleothems as recorded by clumped isotope thermometry. *Geochimica et Cosmochimica Acta* 72: 5351–5360.
- An W, Hu X, Garzanti E, Wang J–G & Liu Q 2021. New precise dating of the India–Asia collision in the Tibetan Himalaya at 61 Ma. *Geophysical Research Letters* 48: e2020GL090641. <https://doi.org/10.1029/2020GL090641>.
- Antal JS & Awasthi N 1993. Fossil flora from the Himalayan foot hills of Darjeeling foot–hills of Darjeeling District, West Bengal and its palaeoecological and phytogeographical significance. *Palaeobotanist* 42 (1): 14–60.
- Antal JS & Prasad M 1996a. Some more leaf–impressions from the Himalayan foothills of Darjeeling District, West Bengal, India. *Palaeobotanist* 43: 1–9.
- Antal JS & Prasad M 1996b. Dipterocarpaceous fossil leaves from Ghish River section in Himalayan foot hills near Oodlabari, Darjeeling District, West Bengal. *Palaeobotanist* 43: 73–77.
- Antal JS & Prasad M 1997. Angiospermous fossil leaves from the Siwalik sediments (Middle–Miocene) of Darjeeling District, West Bengal. *Palaeobotanist* 46: 95–104.
- Antal JS & Prasad M 1998. Morphotaxonomic study of some more fossil leaves from the lower Siwalik sediments of West Bengal, India. *Palaeobotanist* 47: 86–98.
- Antonelli A, Kissling WD, Flantua SGA, Bermúdez MA, Mulch A, Muellner–Riehl AN, Kreft H, Linder PL, Badgley C, Fjeldså J, Fritz SA, Rahbeck C, Herman F, Hooghiemstra H & Hoorn C 2018. Geological and climatic influences on mountain biodiversity. *Nature Geosciences* 11: 718–725.
- Armstrong HA, Wagner T, Herringshaw LG, Farnsworth AJ, Lunt DJ, Harland M, Imber J, Lopston C & Atar EFL 2016. Hadley circulation and precipitation changes controlling black shale deposition in the Late Jurassic Boreal Seaway. *Palaeoceanography* 31: 1041–1053.
- Awasthi N 1992. Changing patterns of vegetation through Siwalik succession. *Palaeobotanist* 40: 312–327.
- Axelrod DI 1981. Altitudes of Tertiary forests estimated from palaeotemperature. *In: Liu DS (Editor)–Proceedings of Symposium on Qinghai–Xizang (Tibet) Plateau, (Beijing, China); Geological and Ecological Studies of Qinghai–Xizang Plateau; vol. 1, Geology, Geological History and Origin of Qinghai–Xiang Plateau. Beijing: Science Press and New York: Gordon and Breach, Science Publishers, Inc.: 131–137.*
- Axelrod DI 1997. Palaeoelevation estimates from Tertiary floras. *International Geology Review* 39: 1124–1133.
- Axelrod DI & Bailey HP 1976. Tertiary vegetation, climate, and altitude of the Rio Grande depression, New Mexico–Colorado. *Paleobiology*: 235–254.
- Banerjee M 1996. Tropical estuarine angiosperm vegetation in the Neogene sediments of Bhutan, Eastern Himalaya, and remarks on palaeogeography of Siwalik foreland basins of Indian Subcontinent. *Rheedea* 6 (1): 127–140.
- Banerjee M & Dasgupta R 1984. Angiosperm leaf remains from the Siwalik sediments (Mio–Pliocene) of Bhutan, Eastern Himalaya. A.K. Ghosh commemorative volume. *Evolutionary Botany and Biostratigraphy*: 129–143.
- Banerjee M & Dasgupta R 1996. Palynostratigraphy and palaeoenvironment–palaeogeographic considerations of Siwalik sediments of Bhutan, Eastern Himalaya. *Geological Survey of India Special Publication* 21 (1): 233–248.
- Bhatia H, Khan MA, Srivastava G, Hazra T, Spicer RA, Mehrotra RC, Spicer TEV, Bera S & Roy K 2021a. Late Cretaceous–Paleogene Indian monsoon climate vis–à–vis movement of the Indian Pplate and the birth of the South Asia Monsoon. *Gondwana Research* 93: 89–100. [https://authors.elsevier.com/sd/article/S1342–937X\(21\)00028–9](https://authors.elsevier.com/sd/article/S1342–937X(21)00028–9).
- Bhatia H, Srivastava G, Spicer RA, Farnsworth A, Spicer TEV, Mehrotra RC, Paudyal K & Valdes PJ 2021b. Leaf physiognomy records the Miocene intensification of the South Asia Monsoon. *Global and Planetary Change* 196: 103365. <https://doi.org/10.1016/j.gloplacha.2020.103365>.
- Boos WR & Kuang Z 2010. Dominant control of the South Asian monsoon by orographic insulation versus plateau heating. *Nature* 463: 218–222.
- Cautley PT 1835. Letter noticing the discovery of further fossils in vast quantity in the Siwalik Range. *Journal of the Asiatic Society of Bengal* 4: 585–587.
- Chatterjee S & Scotese CR 2010. The wandering Indian Plate and its changing biogeography during the Late Cretaceous–Early Tertiary Period. *In: Bandopadhyay S (Editor)–New Aspects of Mesozoic Biogeography. Springer, Berlin, pp 105–126*
- Chatterjee S, Goswami A & Scotese CR 2013. The longest voyage: Tectonic, magmatic, and palaeoclimatic evolution of the Indian Plate during its northward flight from Gondwana to Asia. *Gondwana Research* 23: 238–267. <https://doi.org/10.1016/j.gr.2012.07.001>
- Chevalier M, Cheddadi R & Chase BM 2014. CREST (Climate REconstruction SofTware): a probability density function (PDF)–based quantitative climate reconstruction method. *Climate of the Past* 10: 2081–2098. <https://doi.org/10.5194/cp–10–2081–2014>, 2014.
- Claussen M, Fohlmeister J, Ganopolsky A & Brokin V 2006. Vegetation dynamics amplifies precessional forcing. *Geophysical Research Letters* 33: L09709.
- Clift PD 2017. Cenozoic sedimentary records of climate–tectonic coupling in the Western Himalaya. *Progress in Earth and Planetary Science* 4: 39.
- Clift PD, Carter A, Wysocka A, Long HV, Zheng H & Neubeck N 2020. A late Eocene–Oligocene through–flowing river between the upper Yangtze and south China sea. G–cubed. <https://doi.org/10.1029/2020GC009046>.
- Clift PD, Hodges KV, Heslop D, Hannigan R, Van Long H & Calves G 2008. Correlation of Himalayan exhumation rates and Asian monsoon intensity. *Nature Geoscience* 1: 875–880.

- Coutand I, Whipp D, Grujic D, Bernet M, Fellin M, Bookhagen B, Landry K, Ghalley S & Duncan C 2014. Geometry and kinematics of the main Himalayan thrust and Neogene crustal exhumation in the Bhutanese Himalaya derived from inversion of multithermochronologic data. *Journal of Geophysical Research Solid Earth* 119: 1446–1481.
- Coutand I, Barrier L, Govin G, Grujic D, Hoorn C, Dupont–Nivet G & Najman Y 2016. Late Miocene–Pleistocene evolution of India–Eurasia convergence partitioning between the Bhutan Himalaya and the Shillong Plateau: new evidences from foreland basin deposits along the Dungsam Chu section, eastern Bhutan. *Tectonics* 35: 2963–2994.
- Currie BS, Polissar PJ, Rowley D, Ingals M, Li S, Olack G & Freeman KH 2016. Multiproxy palaeoaltimetry of the late Oligocene–Pliocene Oiyug Basin, southern Tibet. *American Journal of Sciences* 316: 401–436.
- Ding L, Kapp P & Wan X 2005. Paleocene–Eocene record of ophiolite obduction and initial India–Asia collision, south central Tibet. *Tectonics* 24: TC3001
- Ding L, Spicer RA, Yang J, Xu Q, Cai F, Li S, Lai Q, Wang H, Spicer TEV, Yue Y, Shukla A, Srivastava G, Khan MA, Bera S & Mehrotra RC 2017. Quantifying the rise of the Himalaya orogen and implications for the South Asian monsoon. *Geology* 45: 215–218.
- Ding L, Xu Q, Yue YH, Wang HQ, Cai FI & Li SQ 2014. The Andean–type Gangdese mountains: palaeoelevation record from the Paleocene–Eocene Linzhou Basin. *Earth and Planetary Science Letters* 392: 250–264.
- Ding W–N, Ree RH, Spicer RA & Xing W–W 2020. Ancient orogenic and monsoon–driven assembly of the world's richest temperate alpine flora. *Science* 369: 578–581. <https://doi.org/10.1126/science.abb4484>
- Eiler JM 2007. “Clumped–isotope” geochemistry—The study of naturally–occurring, multiply–substituted isotopologues. *Earth and Planetary Science Letters* 262: 309–327. doi: 10.1016/j.epsl.2007.08.020.
- Eiler JM 2011. Paleoclimate reconstruction using carbonate clumped isotope thermometry. *Quaternary Science Reviews* 30: 3575–3588.
- Fang X, Dupont–Nivet G, Wang C, Song C, Meng Q, Zhang W, Nie J, Zhang T, Mao Z & Chen Y 2020. Revised chronology of central Tibet uplift (Lunpola Basin). *Science Advances* 6: eaaba7298.
- Farnsworth A, Lunt DJ, Robinson SA, Valdes PJ, Roberts WHG, Cliff PD, Markwick PJ, Su, T., Wrobel N, Bragg F, Kelland S–J & Pancost RD 2019. Past East Asian monsoon evolution controlled by palaeogeography, not CO<sub>2</sub>. *Science Advances* 5: eaax1697.
- Farnsworth A, Valdes PJ, Spicer RA, Ding L, Witkowski C, Lauretano V, Li S–F, Li S–H & Zhou Z–K 2021. Palaeoclimate model–derived thermal lapse rates: towards increasing precision in palaeoaltimetry studies. *Earth and Planetary Science Letters* 564: 116903 <https://doi.org/10.1016/j.epsl.2021.116903>
- Ferguson DK 1985. The origin of leaf–assemblages—new light on an old problem. *Review of Palaeobotany and Palynology* 46: 117–188.
- Fick SE & Hijmans RJ 2017. WorldClim2: New 1–km spatial resolution climate surfaces for global land surfaces. *International Journal of Climatology* 37: 4302–4315.
- Flohn H 1968. Contributions to a meteorology of the Tibetan Highlands. *Atmospheric Science Papers*. Department of Atmospheric Science, Colorado State University: 130 pp.
- Forest CE, Molnar P & Emanuel KA 1995. Palaeoaltimetry from energy conservation principles. *Nature* 374: 347–350.
- Forest CE, Wolfe JA & Emanuel KA 1999. Palaeoaltimetry incorporating atmospheric physics and botanical estimates of paleoclimate. *Geological Society of America Bulletin* 111: 497–511.
- Gallagher TM & Sheldon ND 2016. Combining soil water balance and clumped isotopes to understand the nature and timing of pedogenic carbonate formation. *Chemical Geology* 435: 79–91. <http://dx.doi.org/10.1016/j.chemgeo.2016.04.023>
- Ghosh P, Adkins J, Affek H, Balta B, Guo W, Schauble E, Schrag D & Eiler J 2006. <sup>13</sup>C–<sup>18</sup>O bonds in carbonate minerals: A new kind of paleothermometer. *Geochimica et Cosmochimica Acta* 70: 1439–1456.
- Gourbet L, Leloup PH, Paquette J–L, Sorrel P, Maheo G, Wang G–C, Xu Y, Cao K, Antoine P–O, Eymard I, Liu W, Lu H, Replumaz A, Chevalier M–L, Zhang K, Wu J & Shen T 2017. Reappraisal of the Jianchuan Cenozoic basin stratigraphy and its implications on the SE Tibetan Plateau evolution. *Tectonophysics* 700–701: 162–179.
- Greenwood DR, Archibald SB, Mathewes RW & Moss PT 2005. Fossil biotas from the Okanagan Highlands, southern British Columbia and northeastern Washington State: climates and ecosystems across an Eocene landscape. *Canadian Journal of Earth Sciences* 42: 167–185.
- Greenwood DR, Moss P, Rowett A., Vadala AJ & Keefe R 2003. Plant communities and climate change in Southeastern Australia during the Early Paleogene. *Geological Society of America Special Paper* 369: 365–380.
- Gregory KM 1994. Paleoclimate and paleoelevation of the 35 Ma Florissant flora, Front Range, Colorado. *Palaeoclimates* 1: 23–57.
- Gregory KM & Chase CG 1992. Tectonic significance of palaeobotanically estimated climate and altitude of the late Eocene erosion surface, Colorado. *Geology* 20: 581–585.
- Gregory KM & McIntosh WC 1996. Paleoclimate and paleoelevation of the Oligocene Pitch Pinnacle flora, Sawatch Range, Colorado. *Geological Society of America Bulletin* 108: 545–561.
- Grossiord C, Buckley TN, Cernusak LA, Novick KA, Poulter B, Siegwolf RTW, Sperry JS & McDowell NG 2020. Plant responses to rising vapour deficit. *New Phytologist* 226: 1550–1566. <https://doi.org/10.1111/nph.16485>
- Ha K–J, Moon S, Timmermann A & Kim D 2020. Future changes of summer monsoon characteristics and evaporative demand over Asia in CMIP6 simulations. *Geophysical Research Letters* 47: e2020GL087492. <https://doi.org/10.1029/2020GL087492>.
- Hazra T, Spicer RA, Hasra M, Mahato S, Spicer TEV, Bera S, Valdes PJ, Farnsworth F, Hughes AC, Yang J & Khan MA 2020. Latest Neogene monsoon of the Chotanagpur Plateau, eastern India, as revealed by fossil leaf architectural signatures. *Palaeogeography, Palaeoclimatology, Palaeoecology* 545: 109641 <https://doi.org/10.1016/j.palaeo.2020.109641>
- He H–Y, Sun J, Li Q & Zhu R 2012. New age determination of the Cenozoic Lunpola Basin, central Tibet. *Geological Magazine* 149(1): 141–145.
- Hetzl R, Dinkl I, Haider V, Strobl M, von Eynatten H, Ding L & Frei D 2011. Peneplain formation in southern Tibet predates the India–Asia collision and plateau uplift. *Geology* 39: 983–986.
- Hoke GD 2018. Geochronology transforms our view of how Tibet's southeast margin evolved. *Geology* 46: 95–96.
- Hoke GD, Liu–Zeng J, Hren MT, Wissink GK & Garzione CN 2014. Stable isotopes reveal high southeast Tibetan Plateau margin since the Paleogene. *Earth Planet Science Letters* 394: 270–278.
- Huber BT & Goldner A 2012. Eocene monsoons. *Journal of Asian Earth Sciences* 44: 3–23.
- Huntington KW, Saylor J, Quade J & Hudson AM 2015. High late Miocene–Pliocene elevation of the Zhada Basin, southwestern Tibetan Plateau, from carbonate clumped isotope thermometry. *GSA Bulletin* 127: 181–199.
- Jain AK, Lal N, Sulemani B, Awasthi AK, Singh S & Kumar D 2009. Detrital–zircon fission–track ages from the lower Cenozoic sediments, Northwestern Himalayan Foreland Basin: clues for exhumation and denudation of the Himalaya during the India–Asia collision. *Geological Society of America Bulletin* 121: 519–535.
- Kapp P & DeCelles PG 2019. Mesozoic–Cenozoic geological evolution of the Himalayan–Tibetan orogen and working tectonic hypotheses. *American Journal of Sciences* 319: 159–254.
- Kershaw AP 1996. A bioclimatic analysis of Early to Middle Miocene brown coal floras, Latrobe Valley, southeastern Australia. *Australian Journal of Botany* 45: 373–383.
- Kershaw AP & Nix HA 1988. Quantitative palaeoclimatic estimates from pollen data using bioclimatic profiles of extant taxa. *Journal of Biogeography* 15: 589–602.
- Khan MA & Bera S 2014a. On some Fabaceous fruits from the Siwalik sediments (Middle Miocene–Lower Pleistocene) of Eastern Himalaya. *Journal of the Geological Society of India* 83: 165–174.
- Khan MA & Bera S 2014b. New lauraceous species from the Siwalik forest of Arunachal Pradesh, eastern Himalaya, and their palaeoclimatic and palaeogeographic implications. *Turkish Journal of Botany* 38: 453–464.
- Khan MA, Bera M, Spicer RA, Spicer TEV & Bera S 2019. Palaeoclimatic estimates for the late Cenozoic (Mio–Pliocene) Siwalik flora of Bhutan:

- Evidence for the development of the South Asian Monsoon in the eastern Himalaya. *Palaeogeography, Palaeoclimatology, Palaeoecology* 514: 326–335.
- Khan MA, Bera S, Ghosh R, Spicer RA & Spicer TEV 2015. Leaf cuticular morphology of some angiosperm taxa from the Siwalik sediments (middle Miocene to lower Pleistocene) of Arunachal Pradesh, eastern Himalaya: systematic and palaeoclimatic implications. *Review of Palaeobotany and Palynology* 214: 9–26.
- Khan M, Bera M, Spicer RA, Spicer TEV & Bera S 2017. First occurrence of mastixioid (Cornaceae) fossil in India and its biogeographic implications. *Review of Palaeobotany and Palynology* 247: 83–96.
- Khan M, Ghosh R, Bera S, Spicer RA & Spicer TEV 2011. Floral diversity during Plio–Pleistocene Siwalik sedimentation (Kimin Formation) in Arunachal Pradesh, India, and its palaeoclimatic significance. *Palaeobiodiversity and Palaeoenvironments* 91: 237–255.
- Khan MA, Spicer RA, Bera S, Ghosh R, Yang J, Spicer TEV, Guo S–X, Su T, Jacques FMB & Grote PJ 2014. Miocene to Pleistocene floras and climate of the eastern Himalayan Siwaliks, and new palaeoelevation estimates for the Namling–Oiyug Basin, Tibet. *Global and Planetary Change* 113: 1–10.
- Khan M, Spicer RA, Spicer TEV & Bera S 2016. Occurrence of *Shorea* Roxburgh ex C. F. Gaertner (Dipterocarpaceae) in the Neogene Siwalik forests of eastern Himalaya and its biogeography during the Cenozoic of Southeast Asia. *Review of Palaeobotany and Palynology* 233: 236–254.
- Khan MA, Spicer RA, Spicer TEV & Bera S 2017. Evidence for diversification of *Calophyllum* L. (Calophyllaceae) in the Neogene Siwalik forests of eastern Himalaya. *Plant Systematics and Evolution* 303: 371–386.
- Khan MA, Spicer RA, Spicer TEV, Roy K, Bera M, Hazra T, Mahato S & Bera S 2020. *Dipterocarpus* Gaertn. (Dipterocarpaceae) leaves from the K–Pg of India: A Cretaceous Gondwana origin of the Dipterocarpaceae. *Plant systematics and evolution* 306: 90 <https://doi.org/10.1007/s00606-020-01718-z>
- Khan SD, Walker DJ, Hall SA, Burke KC, Shah MT & Stockli L 2009. Did the Kohistan–Ladakh Island Arc collide first with India. *Geological Society of America Bulletin* 121: 366–384.
- Kovach W & Spicer RA 1996. Canonical correspondence analysis of leaf physiognomy: a contribution to the development of a new palaeoclimatological tool. *Palaeoclimates: Data and Modelling* 2: 125–138.
- Leuschner DC & Sirocko F 2003. Orbital insolation forcing of the Indian Monsoon—a motor for global climate changes? *Palaeogeography, Palaeoclimatology, Palaeoecology* 197: 83–95.
- Li S, Currie BS, Rowley DB & Ingalls M 2015. Cenozoic palaeoaltimetry of the SE margin of the Tibetan Plateau: constraints on the tectonic evolution of the region. *Earth and Planetary Science Letters* 432: 415–424.
- Li S–H, Su T, Spicer RA, Xu C–L, Sherlock S, Halton A, Hoke G, Tian Y–M, Zhou Z–K, Deng C–L & Zhu R–X 2020. Oligocene deformation of the Chuandian terrane in the SE margin of the Tibetan Plateau related to the extrusion of Indochina. *Tectonics* 39: e2019TC005974.
- Lin J, Dai J–G, Zhuang G, Jia G, Zhang L, Ning Z, Li Y & Wang C 2020. Late Eocene–Oligocene high relief paleotopography in the North Central Tibetan Plateau: Insights from detrital Zircon U–Pb Geochronology and leaf wax hydrogen isotope studies. *Tectonics* 39: e2019TC005815. <https://doi.org/10.1029/2019TC005815>
- Liu X & Yin Z–Y 2002. Sensitivity of East Asian monsoon climate to the uplift of the Tibetan Plateau. *Palaeogeography, Palaeoclimatology, Palaeoecology* 183: 223–245.
- Liu-Zeng J, Zhang J, McPhillips D, Reiners P, Wang W, Pik R, Zeng L, Hoke G, Xie K, Xiao P, Zhen D & Ge Y 2018. Multiple episodes of fast exhumation since Cretaceous in southeast Tibet, revealed by low-temperature thermochronology. *Earth and Planetary Science Letters* 490: 62–76.
- Linnemann U, Su T, Kunzmann L, Spicer RA, Ding W–N, Spicer TEV, Zieger J, Hofmann M, Moraweck K, Gärtner A, Gerdes A, Marko L, Zhang S–T, Li S–F, Tang HL, Huang J, Mulch A, Mosbrugger V & Zhou Z–K 2018. New U–Pb dates show a Paleogene origin for the modern Asian biodiversity hot spots. *Geology* 46: 3–6.
- Liu X–H 2018. Paleoelevation history and evolution of the Cenozoic Lunpola Basin, Central Tibet. PHD thesis, University of the Chinese Academy of Sciences (in Chinese with English abstract).
- Ma P, Wang C, Meng J, Ma C, Zhao X, Li Y & Wang M 2017. Late Oligocene–early Miocene evolution of the Lunpola Basin, central Tibetan Plateau, evidences from successive lacustrine records. *Gondwana Research* 48: 224–236.
- McElwain JC 2004. Climate-independent paleoaltimetry using stomatal density in fossil leaves as a proxy for CO<sub>2</sub> partial pressure. *Geology* 32: 1017–1020.
- Meyer HW 1992. Lapse rates and other variables applied to estimating paleoaltitudes from fossil floras. *Palaeogeography, Palaeoclimatology, Palaeoecology* 99: 71–99.
- Meyer HW 2007. A review of paleotemperature-lapse rate methods for estimating paleoelevation from fossil floras. *Reviews in Mineralogy and Geochemistry* 66: 155–171.
- Molnar P, Boos WR & Battisti DS 2010. Orographic controls on climate and paleoclimate of Asia: thermal and mechanical roles for the Tibetan Plateau. *Annual Review of Earth and Planetary Sciences* 38: 77–102.
- Molnar P & Stock JM 2009. Slowing of India's Convergence with Eurasia since 20 Ma and its Implications for Tibetan Mantle Dynamics Tectonics: 28 TC3001. <https://doi.org/10.1029/2008TC002271>
- Mosbrugger V & Utescher T 1997. The Coexistence Approach—a method for quantitative reconstructions of Tertiary terrestrial palaeoclimate data using plant fossils. *Palaeogeography, Palaeoclimatology, Palaeoecology* 134: 61–86.
- Mulch A 2016. Stable isotope paleoaltimetry and the evolution of landscapes and life. *Earth and Planetary Science Letters* 433: 180–191.
- Mulch A & Chamberlain CP 2006. The rise and growth of Tibet. *Nature* 439: 670–671.
- Mulch A & Chamberlain CP 2018. Stable isotope paleoaltimetry: paleotopography as a key element in the evolution of landscapes and life. *In: Hoorn C, Perrigo A & Antonelli A (Editors)—Mountains, Climate and Biodiversity*. Wiley Blackwell: 81–93.
- Nie J, Ruetenik G, Gallagher K, Hoke GD, Garzzone CN, Wang W, Stockli D, Hu X, Wang Z, Wang Y, Stevens T, Danisik M & Liu S 2018. Rapid incision of the Mekong River in the middle Miocene linked to monsoonal precipitation. *Nature Geoscience* 11: 944–949.
- Polissar P, Freeman K, Rowley D, McInerney F & Currie BS 2009. Paleoaltimetry of the Tibetan Plateau from D/H ratios of lipid biomarkers. *Earth and Planetary Science Letters* 287: 64–76.
- Poole I, Weyers JDB, Lawson T & Raven JA 1996. Variations in stomatal density and index: implications for palaeoclimatic reconstructions. *Plant, Cell and Environment* 19: 705–712.
- Prasad M 1994a. Angiospermous leaf remains from the Siwalik sediments of Haridwar, Uttar Pradesh and their bearing on palaeoclimate and phytogeography. *Himalayan Geology* 15: 83–94.
- Prasad M 1994b. Siwalik (Middle Miocene) woods from the Kalagarh area in the Himalayan foot hills and their bearing on palaeoclimate and phytogeography. *Review of Palaeobotany and Palynology* 76: 49–82.
- Prasad M 1994c. Siwalik (Middle–Miocene) leaf impressions from the foot-hills of the Himalaya, India. *Tertiary Research* 15 (2): 53–90.
- Prasad M & Pandey SM 2008. Plant diversity and climate during Siwalik (Miocene–Pliocene) in the Himalayan foot hills of western Nepal. *Palaeontographica B* 278: 13–70.
- Prasad M & Tripathi PP 2000. Plant megafossils from the Siwalik sediments of Bhutan and their climatic significance. *Biological Memoirs* 26: 6–19.
- Quade J, Eiler J, Daëron M & Achyuthan H 2013. The clumped isotope geothermometer in soil and paleosol carbonate. *Geochimica et Cosmochimica Acta* 105: 92–107. doi: 10.1016/j.gca.2012.11.031.
- Quan C, Liu YS (C) & Utescher T 2011. Paleogene Evolution of Precipitation in northeastern China supporting the middle Eocene intensification of the East Asia Monsoon. *Palaaios* 26: 743–753.
- Rahbeck C, Borregaard MK, Antonelli A, Colwell RK, Holt BG, Nogues-Bravo D, Rasmussen CMØ, Richardson K, Rsoing MT, Whittaker RJ & Fjeldså J 2019. Building mountain biodiversity: geological and evolutionary processes. *Science* 365: 1114–1119.
- Ramage CS 1971. Monsoon Meteorology. International Geophysics Series,

- Vol. 15, Academic Press, San Diego, Calif., 296 pp.
- Reichgelt T, West CK & Greenwood DR 2018. The relation between global palm distribution and climate. *Scientific Reports* 8: 4721–4731.
- Renner SS 2016. Available data point to a 4–km–high Tibetan Plateau by 40 Ma, but 100 molecular–clock papers have linked supposed recent uplift to young node ages. *Journal of Biogeography* 43: 1479–1487.
- Retallack GJ 2005. Pedogenic carbonate proxies for amount and seasonality of precipitation in paleosols. *Geology* 33: 333–336.
- Roperch P & Dupont–Nivet G 2021. Are carbonates from the India–Asia collision remagnetized?, EGU General Assembly 2021, online, 19–30 Apr 2021, EGU21–15842, <https://doi.org/10.5194/egusphere-egu21-15842>, 2021.
- Rowley DB & Currie BS 2006. Palaeoaltimetry of the late Eocene to Miocene Lunpola Basin, central Tibet. *Nature* 439: 677–681. <https://doi.org/10.1038/nature04506>.
- Rowley DB & Garzione CN 2007. Stable isotope–based paleoaltimetry. *Annual Review of Earth and Planetary Sciences* 35: 463–508.
- Rowley D, Pierrehumbert RT & Currie BS 2001. A new approach to stable isotope–based paleoaltimetry; implications for paleoaltimetry and paleohypsometry of the High Himalaya since the late Miocene. *Earth and Planetary Science Letters* 188: 253–268.
- Sahagian DL & Maus JE 1994. Basalt vesicularity as a measure of atmospheric pressure and palaeoelevation. *Nature* 372: 449–451.
- Sahagian, DL, Proussevitch A & Carlson W 2002. Timing of Colorado Plateau uplift: Initial constraints from vesicular basalt–derived palaeoelevations. *Geology* 30: 807–810.
- Sahni A. 1988. Cretaceous–Tertiary boundary events: The fossil vertebrate palaeomagnetic and radiometric evidences from peninsula India. *Journal of Geological Society of India* 32: 382–396.
- Saylor JE, Quade J, Dettman DL, DeCelles PG, Kapp PA & Ding L 2009. The late Miocene through present palaeoelevation history of southwestern Tibet. *American Journal of Sciences* 309: 1–42.
- Song B, Spicer RA, Zhang K, Ji J, Farnsworth A, Hughes AC, Yang Y, Han F, Xu Y, Spicer TEV, Shen T, Lunt DJ & Shi G 2020. Qaidam Basin leaf fossils show northeastern Tibet was high, wet and cool in the early Oligocene. *Earth and Planetary Science Letters* 537: 116175. <https://doi.org/10.1016/j.epsl.2020.116175>
- Spicer RA 2017. Tibet, the Himalaya, Asian monsoons and biodiversity—in what ways are they related? *Plant Diversity* 39: 233–244.
- Spicer RA 2018. *Phytogeography: Using plant fossils to measure past land surface elevation, in mountains, climate and biodiversity*, Hoom C, Perrigo A & Antonelli A (Editors)–(Wiley–Blackwell, 2018), chap. 7: 96–109.
- Spicer RA, Ahlberg A, Herman AB, Hofmann C–C, Raikovich M, Valdes PJ & Markwick PJ 2008. The Late Cretaceous continental interior of Siberia: A challenge for climate models. *Earth and Planetary Science Letters* 267: 228–235.
- Spicer RA, Farnsworth A & Su T 2020a. Cenozoic topography, monsoons and biodiversity conservation within the Tibetan Region: An evolving story. *Plant Diversity* 4: 229–254. <https://doi.org/10.1016/j.pld.2020.06.011>.
- Spicer RA, Harris NBW, Widdowson M, Herman AB, Guo, S, Valdes PJ, Wolfe JA & Kelley SP 2003. Constant elevation of southern Tibet over the past 15 million years. *Nature* 412: 622–624.
- Spicer RA, Su T, Valdes PJ, Farnsworth A, Wu F–X, Shi G, Spicer TEV & Zhou Z–K 2020b. Why the 'uplift of the Tibetan Plateau' is a myth. *National Science Review* 8: nwaa091. <https://doi.org/10.1093/nsr/nwaa091>.
- Spicer RA, Su T, Valdes PJ, Farnsworth A, Wu F–X, Shi G, Spicer TEV & Zhou Z–K 2020c. The topographic evolution of the Tibetan region as revealed by palaeontology. *Palaeobiodiversity and Palaeoenvironments* 101: 213–214. <https://doi.org/10.1007/s12549-020-00452-1>
- Spicer RA & Wolfe JA 1987. Taphonomy of Holocene deposits in Trinity (Clair Engle) Lake, Northern California. *Paleobiology* 13: 227–245.
- Spicer RA, Yang J, Herman A, Kodrul T, Aleksandrova G, Maslova N, Spicer TEV, Ding L, Xu Q, Shukla A, Srivastava G, Mehrotra RC & Jin J–H 2017. Paleogene monsoons across India and South China: drivers of biotic change. *Gondwana Research* 49: 350–363.
- Spicer RA, Yang J, Herman AB, Kodrul T, Maslova N, Spicer TEV, Aleksandrova G & Jin J 2016. Asian Eocene monsoons as revealed by leaf architectural signatures. *Earth and Planetary Science Letters* 449: 61–68.
- Spicer RA, Yang J, Spicer TEV & Farnsworth A 2020d. Woody dicot leaf traits as a palaeoclimate proxy: 100 years of development and application. *Palaeogeography, Palaeoclimatology, Palaeoecology* 562: 110138 <https://doi.org/10.1016/j.palaeo.2020.110138>
- Su T, Farnsworth A, Spicer RA, Huang J, Wu, F–X, Liu J, Li S–F, Xing Y–W, Huang Y–J, Deng W–Y–D, Tang H, Xu C–L, Zhao F, Srivastava G, Valdes PJ, Deng T & Zhou Z–K 2019. No high Tibetan Plateau until the Neogene. *Science Advances* 5: eaav2189.
- Su T, Spicer RA, Li S–H, Xu H, Huang J, Sherlock S, Huang Y–J, Li S–F, Wang L, Jia LB, Deng, W–Y–D, Deng C–L, Zhang S–T, Valdes PJ & Zhou Z–K 2018. Climate and biotic changes at the Eocene–Oligocene transition in south–east Tibet. *National Science Review* 6: 495–504.
- Su T, Spicer RA, Wu F–X, Farnsworth A, Huang J, Deng T, Ding L, Deng W–Y–D, Huang Y–J, Hughes A, Jia L–B, Jin J–H, Li S–F, Liang S–Q, Liu J, Liu X–Y, Sherlock S, Spicer TEV, Srivastava G, Tang H, Valdes PJ, Wang T–X, Widdowson M, Wu M–X, Xing, Y–W, Xu C–L, Yang J, Zhang S–T, Zhang X–W, Zhao F & Zhou Z–K 2020. A middle Eocene lowland humid subtropical 'Shangri–La' ecosystem in central Tibet. *PNAS* 117: 32989–32995. <https://doi.org/10.1073/pnas.2012647117>
- Tanaka T 1954. *Species Problem in Citrus*. Japanese Society for the Promotion of Science. Ueno, Tokyo: 1–15.
- Tang H, Li S–F, Su T, Spicer RA, Zhang S–T, Li S–H, Liu J, Lauretano V, Witkowski C, Spicer TEV, Deng W–Y–D, Wu M–X, Ding WN & Zhou Z–K 2020. Early Oligocene vegetation and climate of southwestern China inferred from palynology. *Palaeogeography, Palaeoclimatology, Palaeoecology* 560: 109988.
- Tian Y, Spicer RA, Huang J, Zhou Z, Su T, Widdowson M, Jia L, Li S, Wu W, Li Xue L, Luo P & Zhang S 2021. Late Paleocene Tectonic deformation and Biodiversity in Yunnan, SW China: new constrains from zircon U–Pb geochronology. *Earth and Planetary Science Letters* 565: 116929. <https://doi.org/10.1016/j.epsl.2021.116929>
- Tuenter E, Weber SL, Hilgen FJ & Lourens LJ 2006. Simulating sub–Milankovitch climate variations associated with vegetation dynamics. *Climate of the Past* 2: 745–769.
- Utescher T, Bruch AA, Erdei B, François L, Ivanov D, Jacques FMB, Kern AK, Liu Y–S(C), Mosbrugger V & Spicer RA 2014. The Coexistence Approach—Theoretical background and practical considerations of using plant fossils for climate quantification. *Palaeogeography Palaeoclimatology Palaeoecology* 410: 58–73.
- Valdes PJ 2000. *Warm climate forcing mechanisms*. Cambridge University Press, Cambridge. 3–20 pp.
- Valdes PJ, Ding L, Farnsworth A, Spicer RA, Li S–H & Su T 2019. Comment on "Revised paleoaltimetry data show low Tibetan Plateau elevation during the Eocene" *Science Technical Comment* 10.1126/science.aax8474..
- van Hinsbergen DJ, Lippert PC, Dupont–Nivet G, McQuarrie N, Doubrovine PV, Spakman W & Torsvik TH 2012. Greater India Basin hypothesis and a two–stage Cenozoic collision between India and Asia. *Proceedings of the National Academy of Sciences* 109(20): 7659–7664.
- Wang B & Ho L 2002. Rainy season of the Asian–Pacific summer monsoon. *Journal of Climate* 15: 386–398.
- Wang CS, Dai J, Zhao X, Li Y, Graham SA, He D, Ran B & Meng J 2014. Outward–growth of the Tibetan Plateau during the Cenozoic: a review. *Tectonophysics*: 621, 1–43.
- Wang E, Kirby E, Furlong KP, van Soest M, Xu G, Shi X, Kamp PJJ & Hodges KV 2012. Two–phase growth of high topography in eastern Tibet during the Cenozoic. *Nature Geoscience* 5(9): 640–645. <https://doi.org/10.1038/ngeo1538>.
- Wang Q, Li Y., Ferguson DK, Mo W–B & Yang N 2021. An equable subtropical climate throughout China in the Miocene based on palaeofloral evidence. *Earth–Science Reviews* <https://doi.org/10.1016/j.earscirev.2021.103649>
- Webster PJ & Fasullo J 2003. Monsoon: dynamical theory. *In: Holton JR (Editor)–Encyclopedia of Atmospheric Sciences*. Academic Press, London, 1370–1385 pp.

- Wei Y, Zhang K, Garzzone CN, Xu Y, Song B & Ji J 2016. Low palaeoelevation of the northern Lhasa terrane during late Eocene: Fossil foraminifera and stable isotope evidence from the Gerze Basin. *Scientific Reports* 6: 27508.
- Wolfe JA 1979. Temperature parameters of humid to mesic forests of eastern Asia and relation to forests of other regions of the Northern Hemisphere and Australasia. United States Geological Survey Professional Paper 1106: 1–37.
- Wolfe JA 1992. An analysis of present-day terrestrial lapse rates in the western conterminous United States and their significance to paleoaltitudinal estimates. *United States Geological Survey Bulletin* 1964: 1–35.
- Wolfe JA 1993. A method of obtaining climatic parameters from leaf assemblages. *United States Geological Survey Bulletin* 2040: 1–73.
- Wu F, Miao D, Chang N–M, Shi G & Wang, N 2017. Fossil climbing perch and associated plant megafossils indicate a warm and wet central Tibet during the late Oligocene. *Scientific Reports* 7: 878–885. <https://doi.org/10.1038/s41598-017-00928-9>.
- Wu Z–Y, Zhou Z–K, Sun H, Li D–Z & Peng H 2006. The areal–types of seed plants and their origin and differentiation. Kunming: Yunnan Publishing Group Corporation Yunnan Science & Technology Press, Kunming: 1–566.
- Xie G, Li J–F, Wang S–Q, Yao Y–F, Sun B, Ferguson DK, Li C–S, Deng T, Liu X–D & Wang Y–F 2021. Bridging the knowledge gap on the evolution of the Asian monsoon during 26–16 Ma, *The Innovation* doi: <https://doi.org/10.1016/j.xinn.2021.100110>.
- Xing Y–W, Utescher T, Jacques FMB, Su T, Liu Y (C), Huang, Y & Zhou Z 2012. Paleoclimatic estimation reveals a weak winter monsoon in southwestern China during the late Miocene: evidence from plant macrofossils. *Palaeogeography Palaeoclimatology Palaeoecology* 358–360: 19–26.
- Xiong Z, Ding L, Wang X, Spicer RA, Farnsworth A, Wang X, Valdes PJ, Su T, Zhang Q, Zhang L, Cai F, Wang H, Li Z, Song P, Guo X & Yue Y 2020. The early Eocene rise of the Gonjo Basin, SE Tibet: from low desert to high forest. *Earth Planetary Science Letters* 543: 116312. <https://doi.org/10.1016/j.epsl.2020.116312>.
- Xu Q, Ding L, Spicer RA, Liu X, Li S & Wang H 2018. Stable isotopes reveal southward growth of the Himalayan–Tibetan Plateau since the Paleocene. *Gondwana Research* 54: 50–61.
- Yanai M & Wu GX 2006. Effects of the Tibetan Plateau. *In: Wang B (Editor)–The Asian Monsoon*. Springer, Berlin, pp. 513–549.
- Yang J, Spicer RA, Spicer TEV, Arens NC, Jacques FMB, Su T, Kennedy EM, Herman AB, Steart DC, Srivastava G, Mehrotra RC, Valdes PJ, Mehrotra NC, Zhou ZK & Lai JS 2015. Leaf form–climate relationships on the global stage: An ensemble of characters. *Global Ecology and Biogeography* 10: 1113–1125.
- Yang J, Spicer RA, Spicer TEV & Li C–S 2011. “CLAMP Online”: a new web-based palaeoclimate tool and its application to the terrestrial Paleogene and Neogene of North America. *Palaeobiodiversity and Palaeoenvironments* 91: 163–183.
- Zaarur S, Olack G & Affek HP 2011. Paleoenvironmental implication of clumped isotopes in land snail shells. *Geochimica et Cosmochimica Acta* 75: 6859–6869. doi: 10.1016/j.gca.2011.08.044.
- Zhang L, Niu H, Wang S, Zhu X, Luo C, Li Y & Zhao X 2012. Gene or environment? Species-specific control of stomatal density and length. *Ecology and Evolution* 2(5): 1965–1070.
- Zhang S & Wang B 2008. Global summer monsoon rainy seasons. *International Journal of Climatology* 28: 1563–1578.
- Zhu J, Poulsen CJ & Tierney JE 2019. Simulation of Eocene extreme warmth and high climate sensitivity through cloud feedbacks. *Science Advances* 5: eaax1874.
- Zhuang GS, Zhang YG, Hourigan JK, Ritts BD, Hren M, Hou MQ, Wu MH & Kim B 2019. Microbial and geochronologic constraints on the Neogene paleotopography of Northern Tibetan Plateau. *Geophysical Research Letters* 46 (3): 1312–1319.